厚生労働科学研究費補助金（創薬基盤推進研究事業）
「パイエル板指向性分子を利用した経口ワクチンの開発」
分担研究報告書

Claudin-4 binder 修飾リポソームの作製

分担研究者　鈴木　亮　　帝京大学薬学部　准教授

研究要旨

Claudin-4（CL-4）に親和性を有するペプチド（C-CPE）を修飾したリポソームを創製した。このリポソームにモデル抗原として ovalbumin（OVA）を封入し、CL-4 発現細胞への特異的な結合性について評価した。その結果、CL-4 に高い親和性を持つ C-CPE 205 (C-CPE04)を修飾したリポソームの CL-4 発現細胞への特異的な結合を確認した。今後、*in vivo* において本リポソームによるパイエル板（PP）への抗原デリバリーについて検討する。

A. 研究目的

インフルエンザウイルスなど感染性病原体の多くは粘膜面を介して生体内に侵入する。現行の多くのワクチンは注射による投与であり、全身免疫を誘導し、生体防御を期待したものである。しかしながら、注射によるワクチン接種法では粘膜免疫を誘導することができず、粘膜からの病原微生物の侵入を防ぐことはできない。一方、粘膜ワクチンは、粘膜免疫と全身免疫の両免疫系を賦活化することができることから、理想的な感染予防・治療法であると言える。

これまでに、当該研究者代表の渡利は、パイエル板をはじめとした粘膜免疫組織に Claudin-4（CL-4）が高発現していることに着目し、CL-4 binder（C-CPE）と抗原の融合たん白質を経鼻投与することで鼻・腸管粘膜面の IgA、血中 IgG 濃度が上昇することを見出し、世界に先駆けて CL-4 binder を利用した経鼻粘膜ワクチン技術の開発に成功している。

経鼻ワクチンでは抗原分子の脳内移行の危険性があることから、患者の生活の質（QOL）およびワクチン活性を考慮すると経口ワクチンが理想的なワクチンである。しかし、精製ワクチン抗原単独を経口投与しても、種々の消化酵素や粘膜を覆う粘液による物理的障壁の影響により、腸管粘膜免疫組織パイエル板（PP）へ抗原を効率よく送達することが困難なことから期待したような抗原特異的な粘膜免疫を誘導することは難しい。これらの問題を克服する試みとして、安全でかつ強力な粘膜免疫誘導が可能な粘膜アジュバントの開発や確実に抗原を誘導組織に送達するデリバリーデバイスの開発が望まれている。

これまでに我々は、脂質二重膜からなる閉鎖小胞であるリポソームを用いた薬物デリバリー技術の開発を行ってきた。がん細胞に標的指向性を持つ分子を修飾したリポソームを調製することで、がん細胞選択的に薬物を送達可能であることを明らかとしている。これらの技術を発展させ、抗原封入型 CL-4 binder 修飾リポソームを開発することで、抗原の消化酵素による分解の回避、PP への抗原の効率的なデリバリーが可能になると考えられ、経口粘膜ワクチンの開発につながると期待される。

本年度は、CL-4 binder 修飾リポソームの調製方法について検討した。また、リポソームにモデル抗原として ovalbumin（OVA）を封入し、CL-4 発現細胞への特異的な結合について検討した。

B. 研究方法

1. C-CPE（CL-4 binder）について

本実験ではアミノ酸配列のことなる 3 種類の C-CPE を使用した。C-CPE194 Y306A/L315A (C-CPE14)は CL-4 に結合性を示さないコントロールペプチドである。

C-CPE 205 (C-CPE04) および C-CPE205 N309A/S313A (C-CPE22) は、CL-4 に特異的に結合するペプチドで、C-CPE22 は C-CPE04 に比べて約 20 倍高い CL-4 親和性を有するペプチドである。

2. C-CPE 修飾 polyethyleneglycol (PEG) リポソームの調製

1,2-Dimyristoyl-sn-glycero-3-phosphocholine (DMPC) : Cholesterol : N-(Carbonyl-methoxypoly ethyleneglycol 2000)-1,2-distearoyl-sn-glycero -3-phosphoethanolamine (DSPE-PEG2k-OMe) : 3-(N-succinimidyloxyglutaryl) aminopropyl, poly ethyleneglycol (2k)-carbamyl distearoylphosphatidyl -ethanolamine (DSPE-PEG2k-NHS) = 50 : 40 : 3 : 3 (モル比) の脂質をエタノール 1.0 mL に溶解した。この脂質エタノール溶液を 10 mL の 9%スクロース溶液にボルテックスミキサーによる撹拌下で注入しリポソームを作製した。その後、extrusion 法で平均粒子径を約 100 nm にした。このリポソームに C-CPE を C-CPE : DSPE-PEG2k-NHS = 1 : 200 となるように混合し、4℃で一晩反応させ C-CPE14, C-CPE04, C-CPE22 をリポソーム表面に修飾した。未反応のポリペプチドは超遠心操作により除去し、その後、凍結乾燥を行った。

3. C-CPE 修飾リポソームの調製

1,2-Distearoyl-sn-glycero-3-phosphocholine (DSPC) : Cholesterol : N-Glutaryl-L-α-phosphatidyl ethanolamine, Distearoyl. (DSPE-Glu) = 63.3 : 31.5 : 5 (モル比) の脂質をクロロホルムに溶解し、NBD で蛍光ラベルした Dipalmitoylphosphatidylethanolamine (NBD-PE) を総脂質量の 1% (モル比) となるように添加した。溶媒を約 60℃の水浴上でロータリーエバポレーターにより減圧留去し、1.5 時間乾燥させ、lipid film を調製した。10 mM MES buffer で再懸濁し、凍結融解を 5 回繰り返し、extrusion 法で平均粒子径を約 600 nm にした。このリポソームに N-hydroxysulfosuccinimede、1-Ethyl-3-(3-dimethylaminopropyl) carbodiimide を加え、DSPE-Glu を活性化した。C-CPE を C-CPE : DSPE-Glu = 1 : 100 となるように混合し、4℃で一晩反応させ、C-CPE14, C-CPE04 をリポソームに修飾した。未反応のペプチドは超遠心操作により除去した。モデル抗原として OVA をリポソームに加え、凍結乾燥した。復水操作により、OVA をリポソームに封入し、OVA 封入 C-CPE 修飾リポソームを調製した。未封入の OVA は超遠心操作により除去した。

4. C-CPE 修飾リポソームの CL-4 発現細胞への結合性評価 (フローサイトメトリー)

マウス繊維芽細胞 (L 細胞) および Claudin-1 (CL-1) もしくは CL-4 遺伝子を導入し CL-1, CL-4 を発現させた L 細胞 (L CL-1, L CL-4) にそれぞれ C-CPE 修飾リポソームを添加し、4℃で 1 時間、NaN_3 (0.1%) 存在下で作用させた。細胞を洗浄後、細胞とリポソームとの結合をフローサイトメトリーにより評価した。

5. C-CPE 修飾リポソームの CL-4 発現細胞への結合性評価 (共焦点顕微鏡)

マウス繊維芽細胞 (L 細胞) および Claudin-1 (CL-1) もしくは CL-4 遺伝子を導入し CL-1, CL-4 を発現させた L 細胞 (L CL-1, L CL-4) をガラスベースディッシュに播種し、CO_2 インキュベーターで 1 日培養した。それぞれの細胞に C-CPE 修飾リポソームを添加し、4℃で 1 時間、NaN_3 (0.1%) 存在下で作用させた。細胞を洗浄後、DAPI で核を染色し、共焦点顕微鏡により観察した。

C. 研究結果

結果は D 項にまとめて記載。

D. 考 察

1. リポソーム内にたん白質等の高分子を封入する方法として凍結乾燥復水法が知られている。これはリポソームを凍結乾燥し、高分子溶液で復水することで、膜の再構成に伴い効率的に高分子がリポソーム内に封入される方法である。そこで、凍結乾燥復水法による C-CPE 修飾 PEG リポソームへの OVA 封入の検討を行った。調製した C-CPE 修飾 PEG リポソームを凍結乾燥した。OVA 溶液による

復水後のリポソームへの OVA 封入率評価および OVA 封入 C-CPE 修飾PEGリポソームの CL-4 発現細胞への結合性評価は研究代表者に依頼した。

2. リポソームに polyethyleneglycol (PEG) を修飾することで血中安定性、滞留性が向上することが知られている。しかしながら、PEG を修飾することにより、リポソームの細胞への取り込みが減少することが報告されている。また、リポソームの粒子径を 400-600 nm 程度にすることで、樹状細胞やマクロファージに効率的に取り込まれることが報告されている。経口ワクチン開発のためには、抗原を効率的に PP へ送達することが重要となる。そこで、PEG を修飾していない粒子径約 600 nm の C-CPE 修飾リポソームの調製を行った。動的散乱法により粒子径を評価し、OVA 封入量については ELISA 法により評価した。その結果、各種 OVA 封入 C-CPE 修飾リポソームの平均粒子径は 600 nm 程度あり (Table 1)、OVA 封入量はおよそ 200 μg/mg lipid であった。今後、復水に使用する OVA 溶液の濃度を検討し、OVA 封入効率の最適化を行う。また、樹状細胞やマクロファージに効率的に取り込まれる C-CPE 修飾リポソームの粒子径や C-CPE 修飾率を検討する予定である。

OVA encapsulating Liposome	Particle size
Non-labeled	612.9 nm
C-CPE14	646.4 nm
C-CPE04	653.5 nm

Table 1. OVA 封入 C-CPE 修飾リポソームの粒子

3. PEG を修飾していない C-CPE 修飾リポソームの CL-4 発現細胞への結合性をフローサイトメトリーにより検討した。その結果、L/CL-4 細胞ではペプチド未修飾リポソームおよび C-CPE14 修飾リポソームと比較し、C-CPE04 修飾リポソーム処理群において、高い蛍光強度が認められた (Fig. 1)。L 細胞および L/CL-1 細胞では、いずれのリポソーム処理群においても顕著な蛍光強度の増大は認められなかった。これらの結果から、PEG を修飾していない C-CPE04 修飾リポソームは CL-4 発現細胞特異的に結合することが明らかとなった。

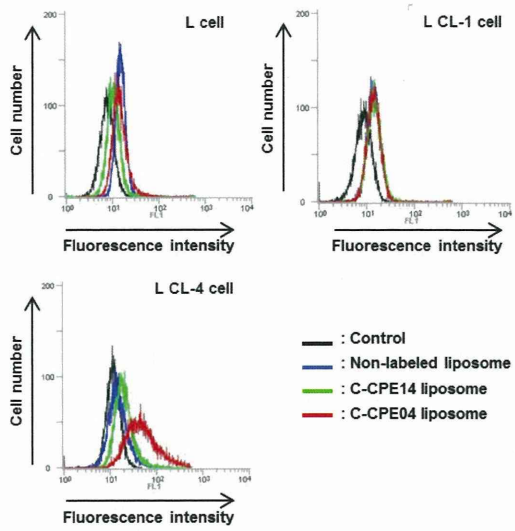

Fig.1. OVA 封入 C-CPE 修飾リポソームの CL-4 発現細胞への結合評価
L, L CL-1, L CL-4 細胞に NBD 標識した各種 OVA 封入 C-CPE 修飾リポソームに添加し、4℃、1 時間培養した。その後、細胞の蛍光をフローサイトメトリーにより測定した。

4. PEG を修飾していない C-CPE 修飾リポソームの L/CL-4 細胞への結合性を共焦点顕微鏡により検討した。その結果、ペプチド未修飾リポソームおよび C-CPE14 修飾リポソーム処理群と比較し、C-CPE04 修飾リポソーム処理群において NBD の蛍光が強く観察された (Fig. 2)。このことから、PEG を修飾していない C-CPE04 修飾リポソームは CL-4 に特異的に結合することが明らかとなった。

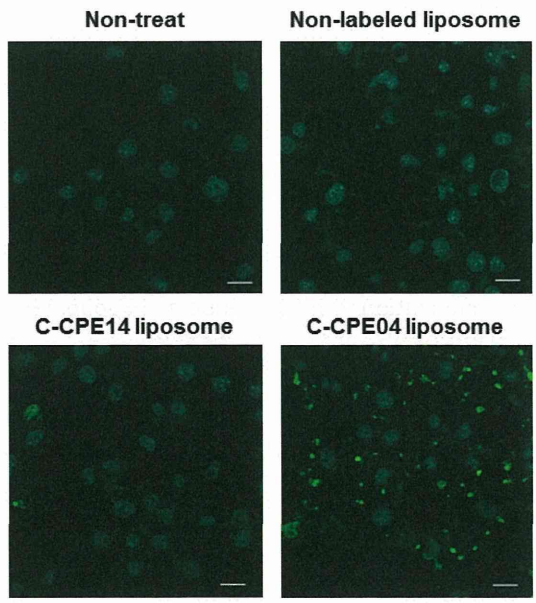

Fig.2. OVA 封入 C-CPE 修飾リポソームの CL-4 発現細胞への結合の観察
L, L CL-1, L CL-4 細胞に NBD 標識した各種 OVA 封入 C-CPE 修飾リポソームに添加し、4℃、1 時間培養した。その後、共焦点顕微鏡による観察を行った。
青:DAPI、緑:NBD、Scale bar:20 μm

E. 結論

CL-4binder を修飾したリポソーム経口ワクチンの開発に向けた基礎的な検討を行った。抗原封入のための凍結乾燥復水操作によるリポソームの粒子径への影響は少ないことが明らかとなった。また、樹状細胞やマクロファージに効率的に抗原をデリバリーするために、PEG を修飾していない粒子径約 600 nm の OVA 封入 CL-4 binder 修飾リポソームを調製した。この CL-4 binder (C-CPE04) 修飾リポソームは CL-4 発現細胞に特異的に結合することをフローサイトメトリーおよび共焦点顕微鏡による検討から明らかとした。今後、OVA 封入効率の最適化、CL-4 binder 修飾率の最適化、および CL-4 に親和性の高い C-CPE22 を用いた検討を進め、*in vivo* での PP への抗原デリバリーについて評価していく予定である。

F. 健康危険情報

なし

G-1 論文発表

1. Omata D, Negishi Y, Yamamura S, Hagiwara S, Endo-Takahashi Y, **Suzuki R**, Maruyama K, Nomizu M, Aramaki Y.: Involvement of Ca2+ and ATP in enhanced gene delivery by bubble liposomes and ultrasound exposure. Mol. Pharm., 9: 1017-1023 (2012)
2. Oda Y, **Suzuki R**, Otake S, Nishiie N, Hirata K, Koshima R, Nomura T, Utoguchi N, Kudo N, Tachibana K, Maruyama k.: Prophylactic immunization with Bubble liposomes and ultrasound-treated dendritic cells provided a four-fold decrease in the frequency of melanoma lung metastasis. J. Control. Release, 160: 362-366 (2012)

G-2 学会発表

1. 澤口能一、小田雄介、小俣大樹、**鈴木 亮**、萩沢康介、丸山一雄、超音波、バブルリポソーム併用血栓溶解療法の基礎的検討、日本薬学会第 133 年会、横浜、3 月 27-30 日
2. 根井彰浩、根岸洋一、高橋佐慧子、小俣大樹、**鈴木 亮**、丸山一雄、野水基義、新槇幸彦、核移行シグナルペプチド内封 AG73 修飾リポソームによる新規遺伝子デリバリーツールの開発、アンチセンス・遺伝子・デリバリーシンポジウム 2012、仙台、2012 年 9 月 24-26 日
3. 小俣大樹、根岸洋一、**鈴木 亮**、丸山一雄、野水基義、新槇幸彦、超音波技術を利用した AG73 修飾 PEG リポソームによる遺伝子導入法の開発、第 21 回 DDS カンファランス、静岡、2012 年 9 月 1 日
4. **Ryo Suzuki**, Yusuke Oda, Daiki Omata, Yoshikazu Sawaguchi, Kazuo Maruyama 、Enhancement of anti-tumor effect by the combination of ultrasound mediated mild hyperthermia and immunotherapy、ICHO&JCTM 2012、京都、2012 年 8 月 28-31 日
5. 根井彰浩、根岸洋一、小俣大樹、山村 翔、高橋葉子、濱野展人、**鈴木 亮**、丸山一雄、新槇幸彦、バブルリポソームと超音波併用によるペプチド修飾リポソームの遺伝子導入増強効果、日本超音波医学会 第 85 回学術集会、2012 年 5 月 25-27 日

H. 知的財産権の出願・登録状況

H-1 特許取得

なし

H-2 実用新案登録

なし

H-3 その他

なし

I. 研究協力者

小田 雄介
平田 圭一
宇留賀 仁史
関 むつみ

研究成果の刊行に関する一覧表

書籍

著者氏名	論文タイトル名	書籍全体の編集者名	書　籍　名	出版社名	出版地	出版年	ページ
	該当事項なし						

雑誌

発表者氏名	論文タイトル名	発表誌名	巻号	ページ	出版年
Watari A, Yagi K, Kondoh M.	A simple reporter assay for screening claudin-4 modulators.	Biochem. Biophys. Res. Commun	426(4)	454-60	2012
Yamagishi Y., Watari A., Hayata Y., Li X., Kondoh M., Tsutsumi Y., Yagi K.	Hepatotoxicity of sub-nanosized platinum particles in mice.	Pharmazie,	68(3)	178-82	2013
Omata D, Negishi Y, Yamamura S, Hagiwara S, Endo-Takahashi Y, Suzuki R, Maruyama K, Nomizu M, Aramaki Y.	Involvement of Ca2+ and ATP in enhanced gene delivery by bubble liposomes and ultrasound exposure.	Mol. Pharm.	9	1017-1023	2012
Oda Y, Suzuki R, Otake S, Nishiie N, Hirata K, Koshima R, Nomura T, Utoguchi N, Kudo N, Tachibana K, Maruyama k.	Prophylactic immunization with Bubble liposomes and ultrasound-treated dendritic cells provided a four-fold decrease in the frequency of melanoma lung metastasis.	J. Control. Release	160	362-366	2012

Biochemical and Biophysical Research Communications 426 (2012) 454–460

Contents lists available at SciVerse ScienceDirect

Biochemical and Biophysical Research Communications

journal homepage: www.elsevier.com/locate/ybbrc

A simple reporter assay for screening claudin-4 modulators

Akihiro Watari, Kiyohito Yagi, Masuo Kondoh *

Laboratory of Bio-Functional Molecular Chemistry, Graduate School of Pharmaceutical Sciences, Osaka University, Suita, Osaka 565-0871, Japan

ARTICLE INFO

Article history:
Received 15 August 2012
Available online 27 August 2012

Keywords:
Claudin
Tight junction
Reporter assay
Screening
Chemical modulator

ABSTRACT

Claudin-4, a member of a tetra-transmembrane protein family that comprises 27 members, is a key functional and structural component of the tight junction-seal in mucosal epithelium. Modulation of the claudin-4-barrier for drug absorption is now of research interest. Disruption of the claudin-4-seal occurs during inflammation. Therefore, claudin-4 modulators (repressors and inducers) are promising candidates for drug development. However, claudin-4 modulators have never been fully developed. Here, we attempted to design a screening system for claudin-4 modulators by using a reporter assay. We prepared a plasmid vector coding a claudin-4 promoter-driven luciferase gene and established stable reporter gene-expressing cells. We identified thiabendazole, carotene and curcumin as claudin-4 inducers, and potassium carbonate as a claudin-4 repressor by using the reporter cells. They also increased or decreased, respectively, the integrity of the tight junction-seal in Caco-2 cells. This simple reporter system will be a powerful tool for the development of claudin-4 modulators.

1. Introduction

Tight junctions (TJs), the most apical components of intercellular junctional complexes, function as fences that maintain cellular polarity and provide a barrier to regulate intercellular permeability of epithelia [1,2]. Disruption of cellular polarity and the TJ-seal is frequently observed during carcinogenesis and inflammation [3]. Modulation of TJ-seals for drug absorption is now of research interest [4,5]. A series of studies has revealed that TJs are composed of transmembrane proteins (such as occludin and claudins), junction adhesion proteins, and cytoplasmic scaffolding proteins, including ZO-1, ZO-2, and ZO-3 (see reviews [6–8]). Of these, claudins are thought to be the main structural and functional components of TJs.

Claudins, tetra-transmembrane proteins with a molecular mass of approximately 23 kDa, comprise a multigene family containing over 20 members [8]. The barrier-function and the expression patterns of claudin members differ among tissues [6,8,9]. Claudin-1-, -5-, and -11-deficient mice show dysfunction of the epidermal barrier, blood–brain barrier, and blood–testis barrier, respectively [10–12]. The expression levels and the barrier-functions of claudins are often altered in various cancer cells; they can be down-regulated or up-regulated, depending on the type of cancer [13]. Changes in claudin expression have also been observed in the mucosal epithelium under inflammatory conditions [14]. Claudins are thus potent targets for drug development, such as drug delivery, anti-cancer agents, and anti-inflammatory agents.

Since claudins play a role in TJ-seals, modulation of the claudin-barrier is a potent strategy for drug absorption. The carboxyl-terminus of *Clostridium perfringens* enterotoxin (C-CPE) is a modulator of the claudin-barrier [15]. Treatment of cells with C-CPE causes a decrease in claudin-4 proteins in TJs, followed by an enhancement of the paracellular transport of solutes without causing cytotoxicity [15]. C-CPE also enhances jejunal, nasal, and pulmonary absorption of drugs [16]. Thus, proof-of-concept for claudin-targeted drug absorption has been demonstrated. A decrease in claudin-4 in the intestinal epithelium often occurs in colitis [17]. Down-regulation of claudin-4 is also observed in some cancer cells [18]. Induction of claudin-4 is involved in the chemo-preventive effect of nonsteroidal anti-inflammatory drugs [19]. A modulator of claudin-4 expression would therefore be a potent molecule for claudin-targeted drug absorption and drug development for some inflammatory diseases and cancers. However, an effective system to screen for claudin modulators is lacking.

Here, we developed a simple system to monitor claudin-4 expression using a reporter gene, and we screened chemical claudin-4 modulators.

Abbreviations: TJs, tight junctions; C-CPE, the carboxyl terminus of *Clostridium perfringens* enterotoxin; TGF-β, transforming growth factor-β; EGF, epidermal growth factor; PMA, phorbol 12-myristate 13-acetate; DMSO, dimethyl sulfoxide; PCR, polymerase chain reaction; RT-PCR, reverse transcription-PCR; GAPDH, glyceraldehyde 3-phosphate dehydrogenase; qPCR, quantitative PCR; SDS, sodium dodecyl sulfate; SDS-PAGE, SDS-polyacrylamide gel electrophoresis; TER, transepithelial electric resistance.

* Corresponding author. Fax: +81 6 6879 8199.
E-mail address: masuo@phs.osaka-u.ac.jp (M. Kondoh).

0006-291X/$ - see front matter © 2012 Elsevier Inc. All rights reserved.
http://dx.doi.org/10.1016/j.bbrc.2012.08.083

2. Materials and methods

2.1. Reagents and cells

Recombinant human transforming growth factor-β (TGF-β) and epidermal growth factor (EGF) were purchased from R&D systems (Minneapolis, MN) and Peprotech Inc. (Rocky Hill, NJ), respectively. The recombinant proteins were dissolved in water and stored at −80 °C before use. Phorbol 12-myristate 13-acetate (PMA) were dissolved in dimethyl sulfoxide (DMSO) and stored at −20 °C before use. List of the chemicals used in this study for screening for claudin-4 modulator is shown in Table 1. All reagents were of research grade.

MCF-7, and Caco-2 cells were cultured in Dulbecco's modified minimal essential medium supplemented with 10% fetal bovine serum in 5% CO_2 at 37 °C. MCF-7 cells were obtained from the RIKEN cell bank (Ibaragi, Japan). Caco-2 cells were obtained from the American Type Culture Collection (Manassas, VA). MCF-7 cells stably expressing snail or HRasV12 were prepared by infection with a recombinant retroviral vector coding for snail or HRasV12 gene.

2.2. Preparation of a reporter plasmid

Genomic DNA was extracted from MCF-7 cells by using a genomic DNA isolation kit (Sigma–Aldrich, St. Louis, MO). The claudin-4 promoter region was cloned by polymerase chain reaction (PCR) using genomic DNA as a template and paired primers (forward primer, 5′-GCGCTAGCGGTTGCCCCCTGGCCTTAAC-3′; reverse primer, 5′-CGCTCGAGGTCCACGGGAGTTGAGGACC-3′). The resultant fragments (500 bp) were subcloned into the pGV-B2 vector encoding the luciferase gene (Toyobo, Osaka, Japan). The sequence of the claudin-4 promoter region was confirmed.

2.3. A transient expression of transfection snail or HRasV12 gene

Transfection was performed with FuGENE HD (Roche, Mannheim, Germany) according to the manufacturer's protocol. Briefly, cells were seeded onto 24-well plates. When the cells reached to 80% confluent cell density, 20 μl of medium containing 0.6 μl of FuGENE HD and 200 ng of plasmid carrying snail or HRasV12 gene was added to the wells. After 48 h of transfection, the luciferase activity of the cell lysates was measured as described below.

2.4. Luciferase assay

Luciferase activity was measured using a commercial available luciferase assay system (Toyo Ink, Tokyo, Japan). Cells were lysed with a cell lysis reagent, LCβ (Toyo Ink). The cell lysates were then centrifuged at *18,000g* for 5 min. The luciferase activity in the resulting supernatant was measured using a TriStar LB 941 microplate reader (Berthold, Wildbad, Germany).

2.5. Establishment of a stable reporter cell line

MCF-7 cells were transfected with the reporter plasmid and a plasmid carrying the puromycin resistance gene. Stable transfectants were selected in the presence of puromycin.

2.6. Screening for claudin-4 modulators

The clone 35 cells were seeded onto 96-well plates at a density of 4×10^4 cells/well. On the following day, vehicle or compound was added, and the cells were cultured for an additional 24 h. The luciferase activity in the cells was then measured as described above.

2.7. Cytotoxicity assay

Clone 35 cells or Caco-2 cells were seeded onto a 96-well plate at a density of 4×10^4 or 6×10^4 cells/well, respectively. On the following day, cells were treated with chemicals at the indicated periods. The cell viability was measured by using a WST-8 assay kit (Nacalai, Kyoto, Japan).

2.8. Reverse transcription–PCR (RT–PCR) analysis

RT reaction and PCR amplification were performed with a cDNA synthesis kit (Roche, Mannheim, Germany) and ExTaqTM (Takara, Shiga, Japan), respectively, according to the manufacturer's instructions. Briefly, total RNA was prepared with TRIzol reagent (Invitrogen, Carlsbad, CA). For reverse transcription, 5 μg of total RNA was used. PCR was performed for 23 cycles for claudin-4 (94 °C for 30 s, 55 °C for 15 s, 72 °C for 30 s) and for 20 cycles for GADPH (94 °C for 30 s, 55 °C for 15 s, 72 °C for 60 s). The PCR products were separated by use of agarose gel electrophoresis and stained with ethidium bromide. The sequences of the primers are as follows: forward primer for claudin-4, 5′-CAACATTGTCACCTCGCAGACCATC-3′; reverse primer for claudin-4, 5′-TATCACCATAAGGCCGGCCAACAG-3′; forward primer for glyceraldehyde 3-phosphate dehydrogenase (GAPDH), 5′-TCTTCACCACCATGGAGAAG-3′; reverse primer for GAPDH, 5′-ACCACCTGGTGCTCAGTGTA-3′.

2.9. Quantitative PCR (qPCR) analysis

qPCR was performed with SYBR Premix Ex Taq II (Takara) using an Applied Biosystems StepOne Plus (Applied Biosystems, Foster City, CA). Relative quantification was performed against a standard curve and the values were normalized against the input determined for the housekeeping gene, GAPDH. The primer sequences used for qPCR were as follows: forward primer for claudin-4, 5′-TTGTCACCTCGCAGACCATC-3′ and reverse primer for claudin-4, 5′-CAGCGAGTCGTACACCTTG-3′; forward primer for GAPDH, 5′-GGTGGTCTCCTCTGACTTCAACA-3′ and reverse primer for GAPDH, 5′-GTGGTCGTTGAGGGCAATG-3′.

2.10. Western blot analysis

Cells were lysed with RIPA buffer (0.15 M NaCl, 50 mM Tris–HCl, pH 7.4, 1 mM ethylenediaminetetraacetic acid, 1% Triton X-100, 1% sodium deoxycholate, 0.1% sodium dodecyl sulfate (SDS), 1% protease inhibitor cocktail [Sigma–Aldrich]). The cell lysates were subjected to 15% SDS–polyacrylamide gel electrophoresis (SDS–PAGE), followed by blotting onto polyvinylidene difluoride membrane. The membranes were incubated with anti-claudin-4 mouse monoclonal (Zymed, South San Francisco, CA) and anti-β-actin mouse monoclonal (Sigma–Aldrich) antibodies, respectively, and subsequently treated with horseradish peroxidase-conjugated anti-mouse IgG (Zymed). The reactive bands were detected by using an enhanced chemiluminescence reagent (GE Healthcare, Buckinghamshire, UK).

2.11. Transepithelial electric resistance (TER) assay

Caco-2 cells were seeded into Transwell™ chambers (Corning, NY) at a density of 8×10^4 cells/well. On 7 days after the seeding or when TER values reached a plateau, claudin-4 inducers (thiabendazole, carotene, or curcumin) or claudin-4 repressor (potassium carbonate), respectively, was added. The TER values were then monitored at 0, 24, and 48 h using a Millicell-ERS epithelial

Table 1
Chemicals used in this study as screening sources.

Sample number	Sample name	Concentration[a]	Relative luciferase activity[b]
1	Tartrazine	10 mM	1.29
2	Potassium nitrate	1 mM	0.94
3	Potassium carbonate	10 mM	0.56
4	Sodium chlorous	10 mM	0.95
5	Zinc sulfate	0.1 mM	0.95
6	New coccine	0.01 mM	0.98
7	Amaranth (Bordeaux S)	1 mM	1.34
8	Allura red AC	1 mM	1.49
9	Sunset yellow FCF	1 mM	1.59
10	Potassium hydroxide	1 mM	0.83
11	L-ascorbic acid	1 mM	1.02
12	Sodium nitrite	10 mM	0.91
13	Propionic acid	0.0001%	0.82
14	Sodium carbonate	1 mM	0.91
15	Zinc gluconate	0.01%	1.76
16	Benzoic acid	0.01 mM	1.3
17	Sorbic acid	1 mM	1.51
18	Aspartame	1 mM	1.59
19	Dibutylhydroxytoluene	0.01 mM	1.81
20	Allyl isothiocyanate	0.0001%	1.72
21	Saccharin	1 mM	1.5
22	L-Ascorbyl palmitate	1 mM	1.21
23	Hydroxy biphenyl	0.01 mM	1.87
24	Aluminium potassium sulfate	0.1 mM	0.94
25	L-Lysine	10 mM	1.42
26	Calcium pantothenate	10 mM	1.61
27	Carrageenin	0.01 mM	1.56
28	Tartaric acid	1 mM	1.01
29	Sodium acetate	10 mM	1.02
30	Glycine	10 mM	1.68
31	Sodium alginate	10 mM	1.52
32	Ammonium chloride	10 mM	1.91
33	Magnesium sulfate	10 mM	1.56
34	5-Ribonucleotide	0.001 mM	1.15
35	Calcium chloride	1 mM	1.62
36	Valine	10 mM	1.08
37	Erythrosine	0.01 mM	1.22
38	Annatto	0.01 mM	1.96
39	Maltitol	10 mM	1.44
40	Sodium dehydroacetate	1 mM	1.98
41	Nicotinic acid	1 mM	1.55
42	Isoleucine	1 mM	1.06
43	Mannitol	10 mM	1.29
44	Ascorbic acid (Vitamin C)	10 mM	1.17
45	Phenylalanine	1 mM	0.95
46	Gallic acid	0.1 mM	1.41
47	Erythorbic acid (Sodium isoascorbate)	1 mM	1.03
48	Magnesium chloride	0.1%	1.26
49	Cochineal extract	0.1%	1.02
50	Calcium dihydrogen pyrophosphate	1 mM	1.1
51	Calcium citrate	0.01 mM	0.92
52	Polyvinyl acetate	0.1 mM	1.13
53	Fumaric acid	0.01 mM	1.24
54	Sodium methyl *p*-hydroxybenzoate	1 mM	2.04
55	Tocophenol (Vitamin E)	0.0001%	2.14
56	Rennet	0.01%	0.89
57	Ionone	0.01%	1.15
58	Isoeugenol	0.001%	1.15
59	Allyl isosulfocyanate	0.001%	1.06
60	Propylene glycol	0.1%	0.87
61	Ethyl isovalerate	0.001%	0.89
62	Pectin	0.001%	0.98
63	Cysteine	0.01 mM	0.76
64	Tragacanth gum	0.01%	0.83
65	Thiamin	0.1%	1.15
66	Gum arabic	0.01%	0.91
67	Cellulose	0.001%	0.84
68	Thiabendazole	0.1 mM	3.24
69	Isopropyl citrate	10 mM	1.04
70	γ-oryzanol	0.01%	1.02
71	Calcium carbonate	0.001%	0.857
72	Propylene glycol alginate	0.01%	0.87
73	Chlorophyll	0.1%	1.02
74	Sodium chondroitin sulfate	0.1%	1.04

Table 1 (*continued*)

Sample number	Sample name	Concentration[a]	Relative luciferase activity[b]
75	Biphenyl	0.1 mM	0.99
76	Sodium cytidylic acid	1 mM	0.77
77	Stevia rebaudiana	0.01%	0.96
78	Calcium stearoyl lactylate	0.01%	0.83
79	Ferrous sulfate	0.1 mM	1.37
80	Calcium sulfate	0.1 mM	0.93
81	Benzoyl peroxide	0.1 mM	1.13
82	Dibenzoyl thiamine	1 mM	0.88
83	Carotene	0.1 mM	2.09
84	Guar gum	0.001%	0.84
85	Xanthan gum	0.001%	0.77
86	Curcumin	0.01 mM	2.0

[a] The chemical concentrations were set at the maximum level to show no cytotoxicity.
[b] The relative luciferase activities were calculated as the ratio of that in the chemical-treated cells to that in the vehicle-treated cells. The treatment period was 24 h.

volt-ohmmeter (Millipore Corporation, Billerica, MA). The TER values were normalized to the area of the Caco-2 cell monolayers, and the TER value of a blank chamber was subtracted.

3. Results

3.1. Preparation of a reporter plasmid encoding a claudin-4-promoter-driven luciferase gene

As a first step toward developing a simple screening system for claudin-4 modulators, we cloned the promoter region of claudin-4. We searched for a region that was highly conserved among animals by using a UCSC Genome Bioinformatics program and cloned a 500 bp fragment corresponding to −293 to +194 bp of the claudin-4 gene. This 500 bp fragment contained various transcription factor-binding sites: an E-box (−276 to −271, −262 to −257, −221 to −216, −19 to −14, +10 to +14), a smad-binding element (SBE; −212 to −209, −103 to −100, −38 to −35), and Sp1 (−66 to −57, −53 to −44) [20,21], indicating that this region is a potent candidate for a regulatory region of claudin-4 expression. We constructed a reporter expression vector, in which the 500 bp fragment was inserted upstream of a luciferase gene Suppl. Fig. 1A). To

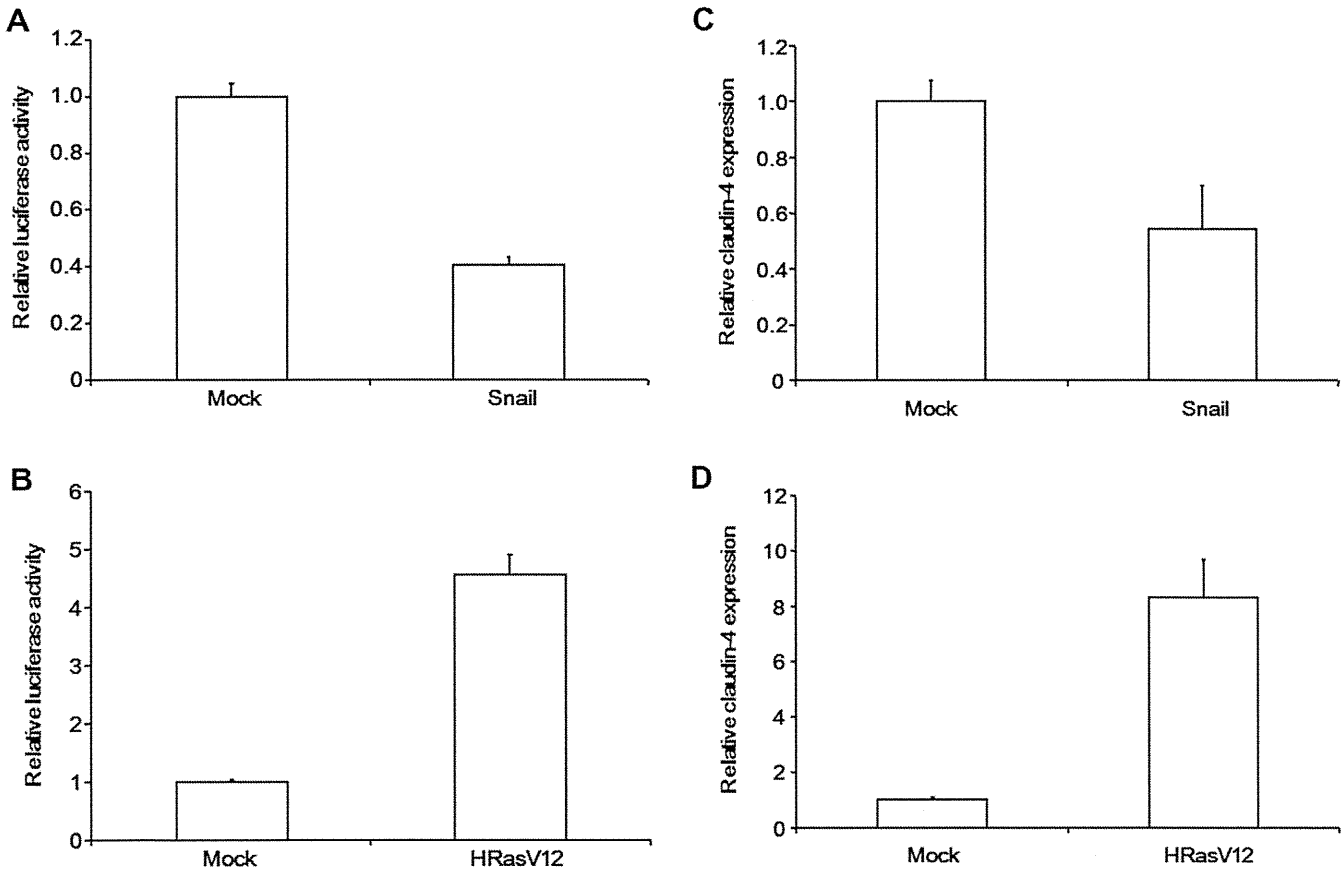

Fig. 1. Preparation of a reporter system monitoring claudin-4 expression. (A, B) Effects of snail and HRasV12 on the luciferase activity in transiently expressing cells. Snail-expressing MCF-7 cells (A) or HRasV12-expressing MCF7 cells (B) were transfected with the claudin-4 reporter plasmid. Two days later, the cells were recovered, and the luciferase activity in the lysates was measured. The data are means ± S.D. ($n = 3$). The results are representative of two independent experiments. (C, D) qPCR analysis of claudin-4 expression in transiently expressing cells. After 2 days of the transfection with the claudin-4 reporter plasmid, total RNA was extracted from snail-expressing MCF-7 cells (C) or HRasV12-expressing MCF-7 cells (D). Expression level of claudin-4 of the transfected cells was quantified by qPCR as described in the Section 2. Claudin-4 expression level was shown as ratio to that of the mock cells. The data are means ± S.D. ($n = 3$). The results are representative of two independent experiments.

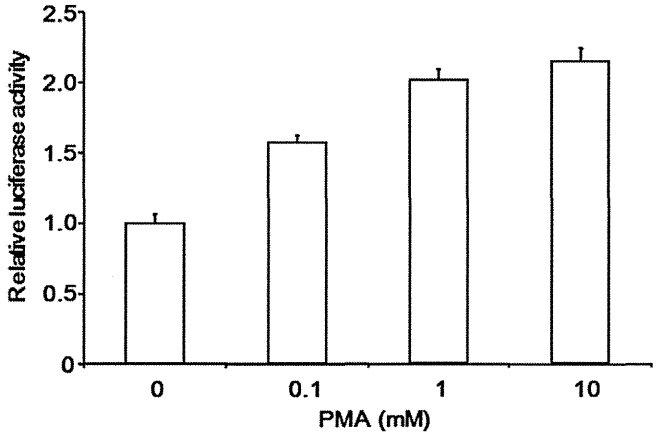

Fig. 2. Effect of PMA on the luciferase activity in clone 35 cells. Clone 35 cells were treated with PMA at the indicated concentrations for 24 h. Luciferase activity in the lysates was measured. The relative luciferase activity is shown as the ratio of the luciferase activity in the treated cells to that of the vehicle-treated cells. The data are means ± S.D. ($n = 3$). The results are representative of two independent experiments.

evaluate expression of the reporter gene, we checked the endogenous claudin-4 expression level in various cell lines and selected MCF-7, HaCat, HT1080, and SiHa cells, which have different claudin-4 expression levels for our analyses (Suppl. Fig. 1B). We transiently transfected the reporter plasmid into these cell lines and found that the luciferase activity of each was correlated with the endogenous expression level of claudin-4 (Suppl. Fig. 1C). We also investigated expression of the reporter gene in MCF-7 cells stably expressing snail or HRasV12, which suppress or induce claudin-4 expression, respectively [22,23]. Transfection of snail- or HRasV12-expressing MCF-7 cells with the reporter plasmid decreased or increased, respectively, the luciferase activity compared to that of mock-transfected MCF-7 cells (Fig. 1A and B). The difference in luciferase activity paralleled the level of claudin-4 mRNA in the cells (Fig. 1C and D), suggesting that the cloned promoter region was functional.

3.2. Preparation of a screening system for claudin-4 modulators

We transfected MCF-7 cells with the claudin-4 reporter plasmid and isolated stable transfected clones. We investigated the effect of transient expression of snail and HRasV12 on luciferase activity in these clones and found that several clones showed altered luciferase activity when transfected with the claudin-4 suppressor (snail, Suppl. Fig. 2A) or the claudin-4 inducer (HRasV12, Suppl. Fig. 2B). TGF-β suppresses claudin-4 expression [23], whereas EGF enhances claudin-4 expression [24]. Therefore, we also investigated the effects of TGF-β and EGF on the luciferase activity in the clones (Suppl. Fig. 2C and D, respectively). Since clone 35 showed the best

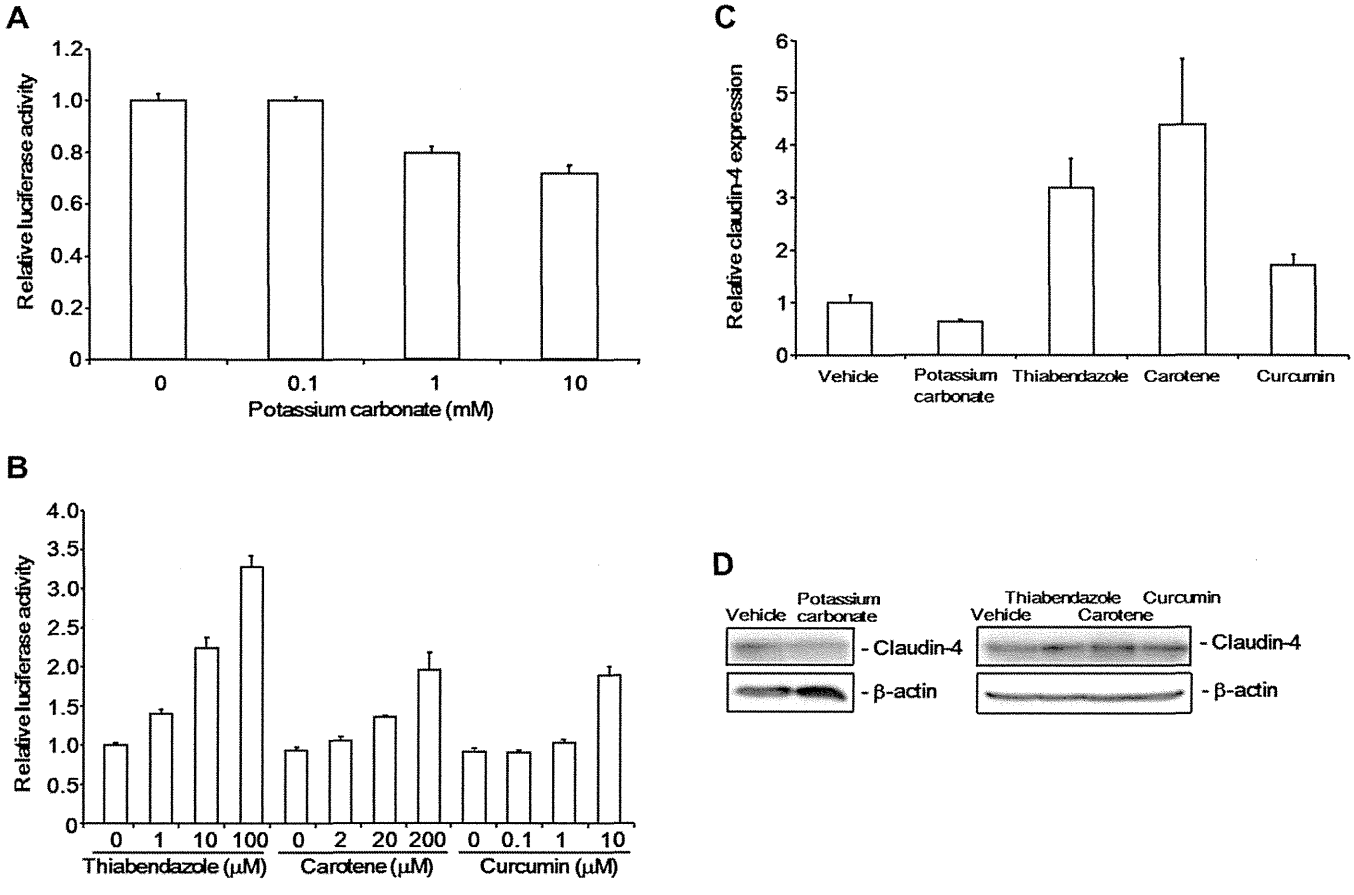

Fig. 3. Screening claudin-4 modulators using the reporter system. (A, B) Dose-dependent effects of the claudin-4 modulator candidates on luciferase expression. Clone 35 cells were treated with potassium carbonate (A), or thiabendazole, carotene, or curcumin (B) at the indicated concentrations for 24 h. Luciferase activity was measured in the lysates. Relative luciferase activity is shown as the ratio of the luciferase activity in the chemical-treated cells to that in the vehicle-treated cells. The data are means ± S.D. ($n = 3$). The results are representative of three independent experiments. (C, D) Effects of the claudin-4 modulator candidates on claudin-4 mRNA expression (C) and claudin-4 protein (D) levels. Clone 35 cells were treated with potassium carbonate (5 mM), thiabendazole (0.1 mM), carotene (0.2 mM), or curcumin (10 μM) for 24 h (C) or 48 h (D). Total RNA was used for qPCR analysis to detect claudin-4 mRNA (C). The relative mRNA expression of claudin-4 normalized to GAPDH expression. The cell lysates were subjected to SDS–PAGE, followed by immunoblotting for claudin-4 (D). GAPDH or β-actin served as loading controls. The result is representative of three independent experiments.

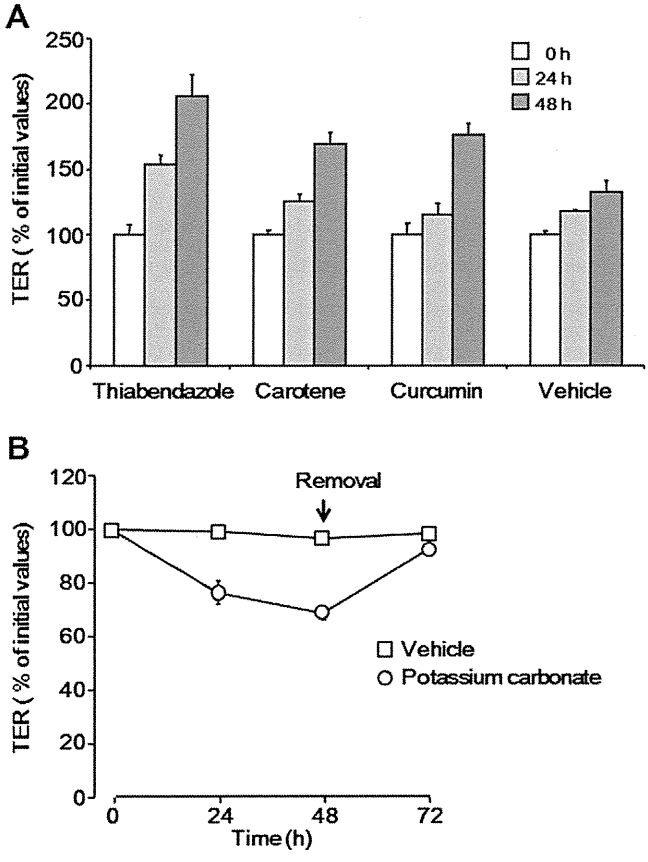

Fig. 4. Effects of claudin-4 modulator on the TJ-barrier in Caco-2 cells. (A) Effect of claudin-4 inducers on the TJ-barrier. Cells were seeded in Transwell™ chambers. Seven days after seeding, the cells were treated with thiabendazole (0.05 mM), carotene (0.2 mM), or curcumin (10 μM). TER values were monitored every 24 h. (B) Effect of a claudin-4 repressor on the TJ-barrier. Cells were seeded in Transwell™ chambers. When the TER values reached a plateau, the TJ-developed cells were treated with potassium carbonate (10 mM). After 48 h of treatment, the medium was replaced with fresh medium. The cells were then cultured for an additional 24 h. TER values were monitored every 24 h. TER values are shown as percentages of the TER values before treatment relative to those in treated cells, as described in the Section 2. The data are means ± S.D. ($n = 3$). These results are representative of three independent experiments.

response to the various claudin-4-modulating treatments, we selected it for further analysis. The clone 35 cells were treated with PMA, which enhances claudin-4 expression [25]. PMA increased luciferase activity in a dose-dependent manner (Fig. 2). These results indicate that clone 35 could be used to screen for modulators of claudin-4 expression.

3.3. Screening for claudin-4 modulators

When we eat, fragments of partially digested food, which still have antigenicity, exist in the intestine. This suggests that claudin modulators that tighten TJ-barriers may be contained in food. Therefore, we screened 86 chemicals used as food additives for claudin-4 modulators (Table 1). At first, we checked the cytotoxicity of these compounds in the clone 35 cells (Table 1). Then, we treated the cells with the compounds at non-toxic concentrations and identified the following claudin-4 modulator candidates: potassium carbonate (No. 3), thiabendazole (No. 68), carotene (No. 83), and curcumin (No. 86) (Suppl. Fig. 3). Each chemical modulated luciferase activity in a dose-dependent manner (Fig. 3A and B). qPCR analysis revealed that thiabendazole, carotene, and curcumin increased claudin-4 expression in the clone 35 cells (Fig. 3C), whereas potassium carbonate decreased claudin-4 expression. Similar results were obtained from Western blot analysis of claudin-4 (Fig. 3D).

To test whether the screened compounds also modulated the TJ-barrier, we investigated the effect of the compounds on the TER value, a marker of TJ-integrity, in Caco-2 cell monolayers, which is a popular model for mucosal barrier. Treatment of cells with thiabendazole, carotene, and curcumin increased the TER values (Fig. 4A). In contrast, potassium carbonate decreased the TER value. Moreover, the TER values recovered when the potassium carbonate was removed (Fig. 4B), and treatment with potassium carbonate did not cause cytotoxicity (data not shown). Thus, we successfully identified claudin-4 modulators.

4. Discussion

Claudin-4 inducers have been the focus of attention in drug development to treat inflammatory diseases and cancers [17–19]; however, their development has been slow. Some chemicals that modulate TJ integrity have been identified: glutamine, bryostatin-1, berberine, quercetin, and butyrate [26–30]. Here, we established a simple monitoring system for claudin-4 expression using a reporter gene, luciferase, and successfully identified chemical claudin-4 modulators: one suppressor of claudin-4 expression, potassium carbonate, and three inducers of claudin-4, thiabendazole, carotene, and curcumin.

Curcumin is an active ingredient of the spice turmeric, which is used in curry powders and as a food preservative. It is also used in traditional medicine to treat various inflammatory conditions, such as arthritis, colitis, and hepatitis [31]. Curcumin has various biological activities, such as anti-inflammatory, anti-oxidant, and anti-cancer effects [32]; however, the underlying mechanisms have never been fully understood. Here, we found that curcumin induces claudin-4 expression and increases TJ integrity. This enhancement of TJ integrity by curcumin may be associated with its therapeutic activities.

Carotene is a precursor of vitamin A. Retinoic acid, a metabolite of vitamin A, enhances TJ integrity in epithelial cells accompanied by expression of claudin-1, -4, and occludin [33]. These findings suggest that metabolized β-carotene-activated expression of claudins enhances the epithelial barrier in Caco-2 cells. Retinoic acid is a biologically active regulator of cell differentiation, proliferation, and apoptosis in various cell types [34]. The activities of retinoic acid are mediated by two types of nuclear receptors: retinoic acid receptors and their heterodimeric counterparts, retinoid X receptors [35]. Specific heterodimer-mediated transcriptional activation increases TJ integrity [36]. The increase in claudin-4 expression and TJ integrity induced by carotene may be caused by the formation of the heterodimer, followed by transcriptional activation.

Thiabendazole is used as a broad spectrum anthelmintic in various animal species and is also used to control parasitic infections in humans [37]. It is also used as an anti-fungal agent for the treatment of fruits [38]. Here, we found that thiabendazole increases claudin-4 expression and TJ integrity, but the mechanism for these activities remains unclear.

Our screening system identified a repressor of intestinal epithelial barrier function as well as three enhancers. We showed that potassium carbonate reduces claudin-4 expression and epithelial barrier function in Caco-2 cells without causing cytotoxicity. Potassium carbonate is used as an acidity regulator, and paracellular permeability is sensitive to pH [39]. Thus, potassium carbonate might reduce epithelial barrier integrity by changing the pH.

In conclusion, we developed the simple screening system for claudin-4 modulator, and we identified several claudin-4 modulators, including three inducers and one repressor. The screening system will thus be a tool for the development of claudin-4

modulators, thereby contributing to basic and pharmaceutical researches.

Acknowledgments

This work was supported by a Grant-in-Aid for Scientific Research from the Ministry of Education, Culture, Sports, Science, and Technology, Japan (21689006; 24390042), by a Health and Labor Sciences Research Grant from the Ministry of Health, Labor, and Welfare of Japan and by the Takeda Science Foundation.

Appendix A. Supplementary data

Supplementary data associated with this article can be found, in the online version, at http://dx.doi.org/10.1016/j.bbrc.2012.08.083.

References

[1] M. Cereijido, R.G. Contreras, L. Shoshani, D. Flores-Benitez, I. Larre, Tight junction and polarity interaction in the transporting epithelial phenotype, Biochim. Biophys. Acta 1778 (2008) 770–793.
[2] D.W. Powell, Barrier function of epithelia, Am. J. Physiol. 241 (1981) G275–288.
[3] A. Wodarz, I. Nathke, Cell polarity in development and cancer, Nat. Cell Biol. 9 (2007) 1016–1024.
[4] B.J. Aungst, Intestinal permeation enhancers, J. Pharm. Sci. 89 (2000) 429–442.
[5] M. Kondoh, T. Yoshida, H. Kakutani, K. Yagi, Targeting tight junction proteins-significance for drug development, Drug Discovery Today 13 (2008) 180–186.
[6] H. Chiba, M. Osanai, M. Murata, T. Kojima, N. Sawada, Transmembrane proteins of tight junctions, Biochim. Biophys. Acta 1778 (2008) 588–600.
[7] L.L. Mitic, V.M. Unger, J.M. Anderson, Expression, solubilization, and biochemical characterization of the tight junction transmembrane protein claudin-4, Protein Sci. 12 (2003) 218–227.
[8] M. Furuse, S. Tsukita, Claudins in occluding junctions of humans and flies, Trends Cell Biol. 16 (2006) 181–188.
[9] K. Morita, M. Furuse, K. Fujimoto, S. Tsukita, Claudin multigene family encoding four-transmembrane domain protein components of tight junction strands, Proc. Natl. Acad. Sci. USA 96 (1999) 511–516.
[10] M. Furuse, M. Hata, K. Furuse, Y. Yoshida, A. Haratake, Y. Sugitani, T. Noda, A. Kubo, S. Tsukita, Claudin-based tight junctions are crucial for the mammalian epidermal barrier: a lesson from claudin-1-deficient mice, J. Cell Biol. 156 (2002) 1099–1111.
[11] A. Gow, C.M. Southwood, J.S. Li, M. Pariali, G.P. Riordan, S.E. Brodie, J. Danias, J.M. Bronstein, B. Kachar, R.A. Lazzarini, CNS myelin and sertoli cell tight junction strands are absent in Osp/claudin-11 null mice, Cell 99 (1999) 649–659.
[12] T. Nitta, M. Hata, S. Gotoh, Y. Seo, H. Sasaki, N. Hashimoto, M. Furuse, S. Tsukita, Size-selective loosening of the blood–brain barrier in claudin-5-deficient mice, J. Cell Biol. 161 (2003) 653–660.
[13] P.J. Morin, Claudin proteins in human cancer: promising new targets for diagnosis and therapy, Cancer Res. 65 (2005) 9603–9606.
[14] J.D. Schulzke, S. Ploeger, M. Amasheh, A. Fromm, S. Zeissig, H. Troeger, J. Richter, C. Bojarski, M. Schumann, M. Fromm, Epithelial tight junctions in intestinal inflammation, Ann. N. Y. Acad. Sci. 1165 (2009) 294–300.
[15] N. Sonoda, M. Furuse, H. Sasaki, S. Yonemura, J. Katahira, Y. Horiguchi, S. Tsukita, *Clostridium perfringens* enterotoxin fragment removes specific claudins from tight junction strands: evidence for direct involvement of claudins in tight junction barrier, J. Cell Biol. 147 (1999) 195–204.
[16] H. Uchida, M. Kondoh, T. Hanada, A. Takahashi, T. Hamakubo, K. Yagi, A claudin-4 modulator enhances the mucosal absorption of a biologically active peptide, Biochem. Pharmacol. 79 (2010) 1437–1444.
[17] R. Mennigen, K. Nolte, E. Rijcken, M. Utech, B. Loeffler, N. Senninger, M. Bruewer, Probiotic mixture VSL#3 protects the epithelial barrier by maintaining tight junction protein expression and preventing apoptosis in a murine model of colitis, Am. J. Physiol. 296 (2009) G1140–1149.
[18] S.K. Lee, J. Moon, S.W. Park, S.Y. Song, J.B. Chung, J.K. Kang, Loss of the tight junction protein claudin 4 correlates with histological growth-pattern and differentiation in advanced gastric adenocarcinoma, Oncol. Rep. 13 (2005) 193–199.
[19] S. Mima, S. Tsutsumi, H. Ushijima, M. Takeda, I. Fukuda, K. Yokomizo, K. Suzuki, K. Sano, T. Nakanishi, W. Tomisato, T. Tsuchiya, T. Mizushima, Induction of claudin-4 by nonsteroidal anti-inflammatory drugs and its contribution to their chemopreventive effect, Cancer Res. 65 (2005) 1868–1876.
[20] H. Honda, M.J. Pazin, H. Ji, R.P. Wernyj, P.J. Morin, Crucial roles of Sp1 and epigenetic modifications in the regulation of the CLDN4 promoter in ovarian cancer cells, J. Biol. Chem. 281 (2006) 21433–21444.
[21] T. Vincent, E.P. Neve, J.R. Johnson, A. Kukalev, F. Rojo, J. Albanell, K. Pietras, I. Virtanen, L. Philipson, P.L. Leopold, R.G. Crystal, A.G. de Herreros, A. Moustakas, R.F. Pettersson, J. Fuxe, A SNAIL1-SMAD3/4 transcriptional repressor complex promotes TGF-beta mediated epithelial–mesenchymal transition, Nat. Cell Biol. 11 (2009) 943–950.
[22] J. Ikenouchi, M. Matsuda, M. Furuse, S. Tsukita, Regulation of tight junctions during the epithelium–mesenchyme transition: direct repression of the gene expression of claudins/occludin by snail, J. Cell Sci. 116 (2003) 1959–1967.
[23] P. Michl, C. Barth, M. Buchholz, M.M. Lerch, M. Rolke, K.H. Holzmann, A. Menke, H. Fensterer, K. Giehl, M. Lohr, G. Leder, T. Iwamura, G. Adler, T.M. Gress, Claudin-4 expression decreases invasiveness and metastatic potential of pancreatic cancer, Cancer Res. 63 (2003) 6265–6271.
[24] A. Ikari, K. Atomi, A. Takiguchi, Y. Yamazaki, M. Miwa, J. Sugatani, Epidermal growth factor increases claudin-4 expression mediated by Sp1 elevation in MDCK cells, Biochem. Biophys. Res. Commun. 384 (2009) 306–310.
[25] C. Wray, Y. Mao, J. Pan, A. Chandrasena, F. Piasta, J.A. Frank, Claudin-4 augments alveolar epithelial barrier function and is induced in acute lung injury, Am. J. Physiol. 297 (2009) L219–227.
[26] L. Gu, N. Li, Q. Li, Q. Zhang, C. Wang, W. Zhu, J. Li, The effect of berberine in vitro on tight junctions in human Caco-2 intestinal epithelial cells, Fitoterapia 80 (2009) 241–248.
[27] N. Li, V.G. DeMarco, C.M. West, J. Neu, Glutamine supports recovery from loss of transepithelial resistance and increase of permeability induced by media change in Caco-2 cells, J. Nutr. Biochem. 14 (2003) 401–408.
[28] L. Peng, Z.R. Li, R.S. Green, I.R. Holzman, J. Lin, Butyrate enhances the intestinal barrier by facilitating tight junction assembly via activation of AMP-activated protein kinase in Caco-2 cell monolayers, J. Nutr. 139 (2009) 1619–1625.
[29] T. Suzuki, H. Hara, Quercetin enhances intestinal barrier function through the assembly of zonula [corrected] occludens-2, occludin, and claudin-1 and the expression of claudin-4 in Caco-2 cells, J. Nutr. 139 (2009) 965–974.
[30] J. Yoo, A. Nichols, J.C. Song, J. Mammen, I. Calvo, R.T. Worrell, J. Cuppoletti, K. Matlin, J.B. Matthews, Bryostatin-1 attenuates TNF-induced epithelial barrier dysfunction: role of novel PKC isozymes, Am. J. Physiol. 284 (2003) G703–712.
[31] J. Epstein, I.R. Sanderson, T.T. Macdonald, Curcumin as a therapeutic agent: the evidence from in vitro, animal and human studies, Br. J. Nutr. 103 (2010) 1545–1557.
[32] R.K. Maheshwari, A.K. Singh, J. Gaddipati, R.C. Srimal, Multiple biological activities of curcumin: a short review, Life Sci. 78 (2006) 2081–2087.
[33] M. Osanai, N. Nishikiori, M. Murata, H. Chiba, T. Kojima, N. Sawada, Cellular retinoic acid bioavailability determines epithelial integrity: role of retinoic acid receptor alpha agonists in colitis, Mol. Pharmacol. 71 (2007) 250–258.
[34] M. Osanai, M. Petkovich, Expression of the retinoic acid-metabolizing enzyme CYP26A1 limits programmed cell death, Mol. Pharmacol. 67 (2005) 1808–1817.
[35] P. Kastner, M. Mark, P. Chambon, Nonsteroid nuclear receptors: what are genetic studies telling us about their role in real life?, Cell 83 (1995) 859–869
[36] H. Kubota, H. Chiba, Y. Takakuwa, M. Osanai, H. Tobioka, G. Kohama, M. Mori, N. Sawada, Retinoid X receptor alpha and retinoic acid receptor gamma mediate expression of genes encoding tight-junction proteins and barrier function in F9 cells during visceral endodermal differentiation, Exp. Cell Res. 263 (2001) 163–172.
[37] K. Walton, R. Walker, J.J. van de Sandt, J.V. Castell, A.G. Knapp, G. Kozianowski, M. Roberfroid, B. Schilter, The application of in vitro data in the derivation of the acceptable daily intake of food additives, Food Chem. Toxicol. 37 (1999) 1175–1197.
[38] J.P. Groten, W. Butler, V.J. Feron, G. Kozianowski, A.G. Renwick, R. Walker, An analysis of the possibility for health implications of joint actions and interactions between food additives, Regul. Toxicol. Pharmacol. 31 (2000) 77–91.
[39] V.W. Tang, D.A. Goodenough, Paracellular ion channel at the tight junction, Biophys. J. 84 (2003) 1660–1673.

Laboratories of Bio-Functional Molecular Chemistry[1] and Toxicology and Safety Science[2], Graduate School of Pharmaceutical Sciences, Osaka University, Japan

Hepatotoxicity of sub-nanosized platinum particles in mice

Y. YAMAGISHI[1], A. WATARI[1], Y. HAYATA[1], X. LI[1], M. KONDOH[1], Y. TSUTSUMI[2], K. YAGI[1]

Received July 19, 2012, accepted August 30, 2012

Dr. Akihiro Watari, Laboratory of Bio-Functional Molecular Chemistry, Graduate School of Pharmaceutical Sciences, Osaka University, Suita, Osaka 565-0871, Japan
akihiro@phs.osaka-u.ac.jp

Pharmazie 68: 178–182 (2013) *doi: 10.1691/ph.2013.2141*

Nano-sized materials are widely used in consumer products, medical devices and engineered pharmaceuticals. Advances in nanotechnology have resulted in materials smaller than the nanoscale, but the biologic safety of the sub-nanosized materials has not been fully assessed. In this study, we evaluated the toxic effects of sub-nanosized platinum particles (snPt) in the mouse liver. After intravenous administration of snPt (15 mg/kg body weight) into mice, histological analysis revealed acute hepatic injury, and biochemical analysis showed increased levels of serum markers of liver injury and inflammatory cytokines. In contrast, administration of nano-sized platinum particles did not produce these abnormalities. Furthermore, snPt induced cytotoxicity when directly applied to primary hepatocytes. These data suggest that snPt have the potential to induce hepatotoxicity. These findings provide useful information on the further development of sub-nanosized materials.

1. Introduction

Nanotechnology involves manipulation of matter on the scale of the nanometer and has the potential to improve quality of life via functional products. Nanomaterials are commonly defined as objects with dimensions of 1 to 100 nm and are now widely used in electronics, catalysts, clothing, drugs, diagnostic devices, and cosmetics (Baughman et al. 2002; Patra et al. 2010; Service et al. 2007; Ariga et al. 2010). Recent progress in the field has allowed the creation of sub-nanosized materials that have different physicochemical properties, including improved conductivity, durability and strength. Although these materials may be useful for industrial and scientific purposes, the biologic safety of these materials has not been fully evaluated (Nel et al. 2006; Oberdorster et al. 2005).

Nano-sized platinum particles (nPt) are used for industrial applications and in consumer products, such as cosmetics, supplements and food additives (Gehrke et al. 2011; Horie et al. 2011). The biological influence of exposure to nPt has been previously investigated. For example, nPt has anti-oxidative activity (Watanabe et al. 2009; Onizawa et al. 2009; Kajita et al. 2007), and may be useful for the medical treatment of diseases related to oxidative stress and aging. However, some reports suggest that these substances can induce inflammation in mice or impair DNA integrity (Pelka et al. 2009; Park et al. 2010). Thus, the understanding of the biological influences of nPt has still not been definitively established, and our knowledge regarding the biological effects of sub-nanosized platinum particles (snPt) is severely lacking.

Nano-sized particles can enter and penetrate the lungs, intestines and skin. The degree of penetration depends on the size and surface features of the nano-sized particle. Furthermore, nanoparticles can enter the circulatory system and migrate to various organs, such as the brain, spleen, liver, kidney and muscles (Zhu et al. 2008; Furuyama et al. 2009; Oberdorster et al. 2004; Ai et al. 2011). The liver is a vital organ that is involved in the uptake of nutrients and the elimination of waste products and pathogens from the blood; it is also an important organ for the clearance of nanoparticles. However, some nanoparticles are hepatotoxic (Nishimori et al. 2009a, b; Ji et al. 2009; Cho et al. 2009; Folkmann et al. 2009). In the present study, we investigated the influence of sub-nanosized platinum particles (snPt) on the liver.

2. Investigations and results

To investigate the acute liver toxicity of snPt, we administered snPt (15 mg/kg body weight) into mice by intravenous injection. Histological analysis revealed acute hepatic injury, including vacuole degeneration (Fig. 1). Furthermore, administration of snPt at doses over 15 mg/kg resulted in significant elevation of serum alanine aminotransferase (ALT) and aspartate aminotransferase (AST) levels (Fig. 2A and B) and of interleukin-6 (IL-6) levels (Fig. 2C). ALT and AST levels were increased at 3 h to 24 h after intravenous administration at 20 mg/kg snPt (Fig. 3A and B). Cell viability assessment by WST assay demonstrated that direct treatment of isolated hepatocytes with snPt at concentrations of 0.1, 1, 10, 50 and 100 μg/ml resulted in a dose-dependent decrease in hepatocyte viability when compared with vehicle-treated cells (Fig. 4). These observations suggest that snPt induced inflammation and hepatocyte death.

Previous reports showed that biological influences of nanomaterials vary according to material size (Nishimori et al. 2009a, b; Jiang et al. 2008; Oberdorster et al. 2010). Therefore, we examined whether nPt, with a diameter of approximately 15 nm, leads

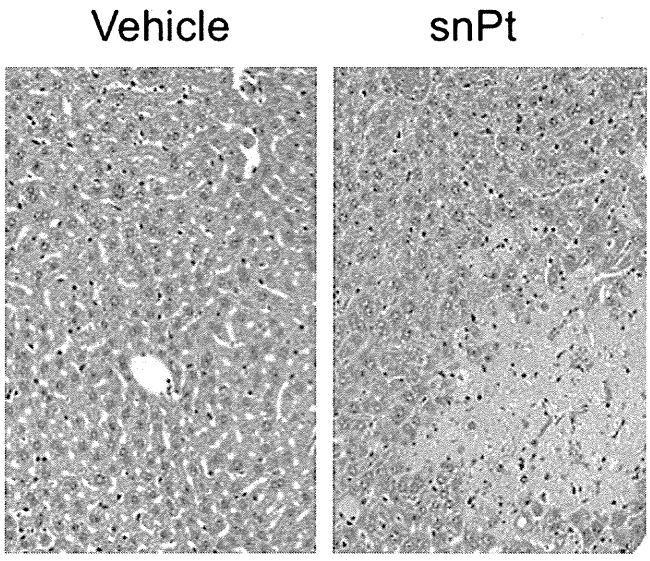

Fig. 1: Histological analysis of liver tissues in snPt-treated mice. snPt was intravenously administered to mice at 15 mg/kg. At 24 h after administration, livers were collected and fixed with 4% paraformaldehyde. Tissue sections were stained with hematoxylin and eosin and observed under a microscope. The pictures show representative data from at least four mice

to a different biologic effect than snPt. As shown in Fig. 5, snPt administration resulted in dose-dependent increases in serum ALT and AST levels, whereas nPt did not. Furthermore, IL-6 levels did not change in response to administration of nPt. These results suggest that the biological effects of platinum particles are dependent on their size.

3. Discussion

The influence of size and of physiochemical properties of nanoparticles on their biologic safety is an important issue. Animal experiments have demonstrated rapid translocation of nanoparticles from the entry site to various organs (Almeida et al. 2011). In particular, nanoparticles tend to concentrate in the liver and are cleared from the body in the feces and urine after intravenous infusion (Ai et al. 2011). While the liver plays a pivotal role in the clearance of nanoparticles, some nanomaterials can induce liver injury. Therefore, we assessed the influence of snPt on the liver and demonstrated that snPt induced liver toxicity *in vitro* and *in vivo*.

Some studies have reported that nPt exert anti-oxidant and anti-inflammatory effects (Watanabe et al. 2009; Onizawa et al. 2009; Kajita et al. 2007), while other studies reported that nPt have negative biological effects. For example, treatment of a human colon carcinoma cell line with nPt resulted in a decrease in cellular glutathione level and impairment in DNA integrity (Pelka et al. 2009). Furthermore, Park et al. (2010) found that nPt prepared from K_2PtCl_6 may induce an inflammatory response in mice. In this study, we found that snPt damaged liver tissues and induced inflammatory cytokines. Kupffer cells present in liver sinusoids may mediate this process via phagocytosis of the particles and subsequent release of inflammatory cytokines. However, when we added snPt to primary hepatocytes, the viability of the cells was significantly reduced, suggesting that snPt may also exert a direct hepatotoxic effect. Thus, the cellular influences of Pt nano- and sub-nano particles may be dependent on the target cells as well as on the size and physical and chemical properties of the particles.

snPt may damage other tissues as well. Cisplatin, a first-line chemotherapy for most cancers, is a platinating agent that can cause kidney damage (Daugaard et al. 1990; Brabec et al. 2005). Furthermore, snPt-induced increases in systemic IL-6 may cause damage to various organs. Further analysis of the distribution and toxic effects of snPt is necessary.

Widespread application of sub-nanosized materials comes with an increased risk of human exposure and environmental release, and the future of nanotechnology will depend on the public acceptance of the risk-benefit ratio. The present study demonstrated that snPt induces hepatotoxicity *in vitro* and *in vivo*. However, our research also indicates that the toxicity of platinum particles could be reduced by altering their size. Additionally, biocompatible coatings can reduce the negative effects of nanoparticles on cells (Oberdorster et al. 2010; Nabeshi et al. 2011; Singh et al. 2007; Clift et al. 2008). Therefore, future studies will contribute to the development of sub-nanosized materials and will also help produce safer products.

4. Experimental

4.1. Materials

Platinum particles with a diameter of 15 nm (nPt) and less than 1 nm (snPt) were purchased from Polytech & Net GmbH (Rostock, Germany). The

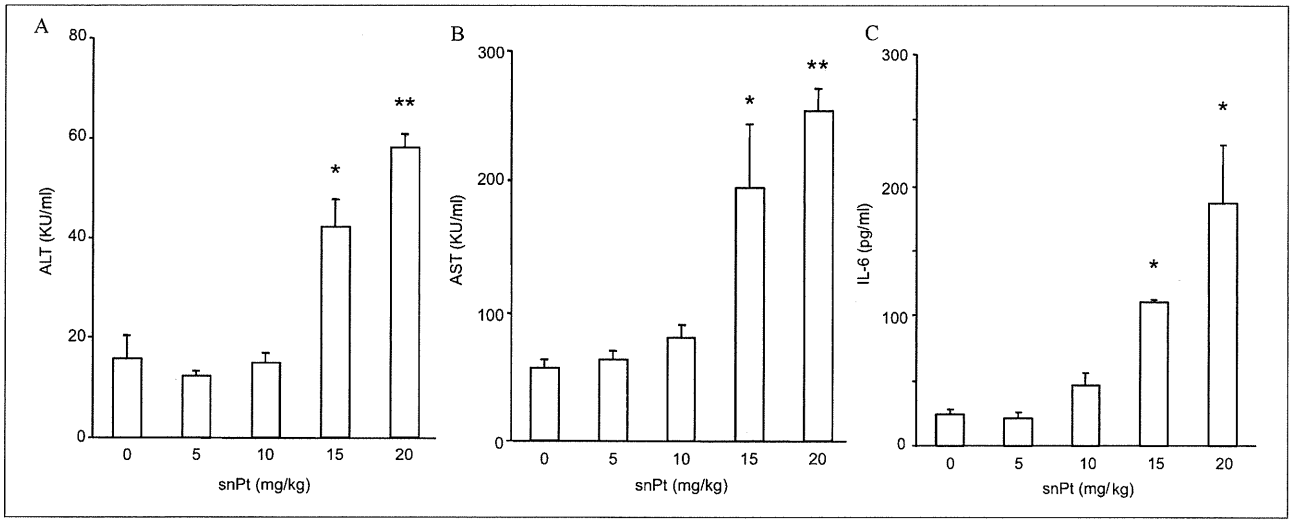

Fig. 2: Dose dependency of snPt-induced liver injury. snPt was intravenously administrated at 5, 10, 15 and 20 mg/kg. At 24 h after administration, blood was recovered, and the resultant serum was used for measurement of ALT (A), AST (B) and IL-6 (C), as described in the "Experimental" section. Data are means ± SEM (n = 3). *Significant difference when compared with the vehicle-treated group (*, $p < 0.05$, **, $p < 0.01$)

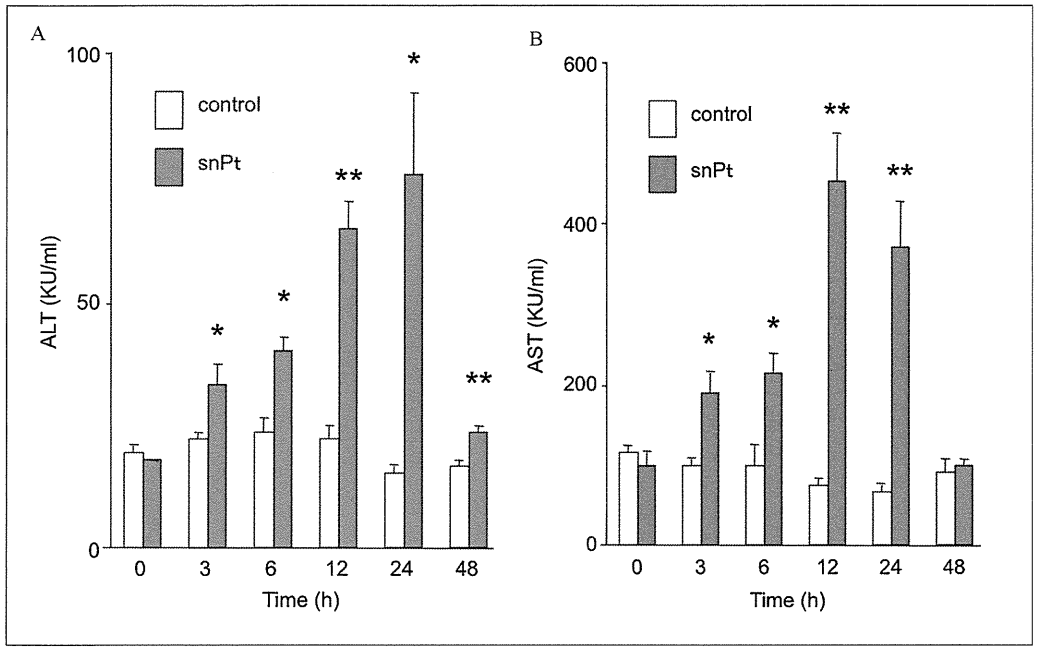

Fig. 3: Time-dependent changes of a biological marker of liver injury. snPt was intravenously administered to mice at 15 mg/kg. Blood was recovered at 3, 6, 12, 24 and 48 h after administration. The serum was used for measurement of ALT (A) and AST (B), as described in the "Experimental" section. Data are means ± SEM (n = 3). *Significant difference when compared with the vehicle-treated group (*, $p < 0.05$, **, $p < 0.01$)

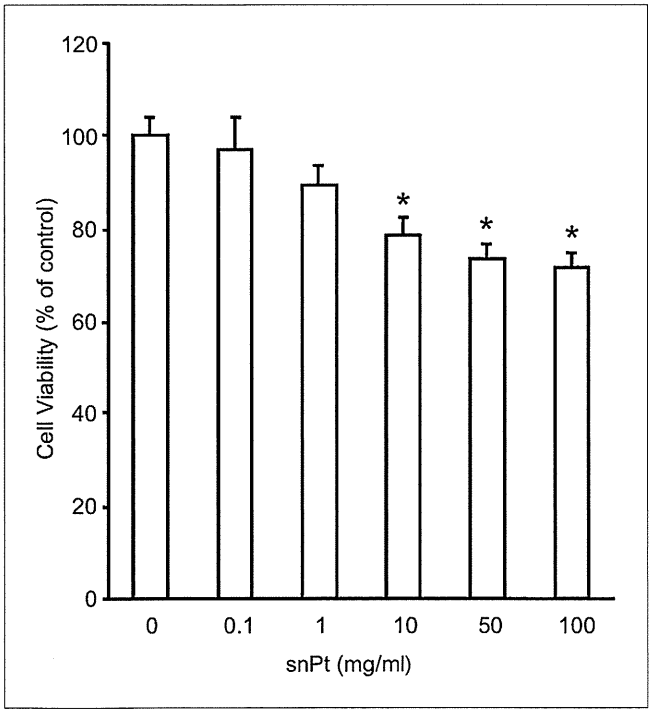

Fig. 4: Cytotoxicity of snPt in hepatic cells. Primary hepatocytes were treated with snPt at 0.1, 1, 10, 50 or 100 μg/ml. After 24 h of culture, cell viability was evaluated with the WST assay, as described in the "Experimental" section. Data are means ± SEM (n = 3). *Significant difference when compared with the vehicle-treated group ($P < 0.05$)

particles were stocked in a 5 mg/ml aqueous suspension. The stock solutions were suspended using a vortex mixer before use. Reagents used in this study were of research grade.

4.2. Animals

BALB/c male mice (8 weeks old) were obtained from Shimizu Laboratory Supplies Co., Ltd. (Kyoto, Japan), and were housed in an environmentally controlled room at 23 ± 1.5 °C with a 12 h light/12 h dark cycle. Mice had access to water and commercial chow (Type MF, Oriental Yeast, Tokyo, Japan). Mice were intravenously injected with nPt or snPt at 5 to 20 mg/kg body weight. The experimental protocols conformed to the ethical guidelines of the Graduate School of Pharmaceutical Sciences, Osaka University.

4.3. Cells

Mouse primary hepatocytes were isolated from BALB/c mice (Shimizu Laboratory Supplies Co.) by the collagenase-perfusion method (Seglen 1976). Isolated hepatocytes were suspended in Williams' E medium containing 10% fetal calf serum, 1 nM insulin, and 1 nM dexamethasone. Next, cell viability was assessed by Trypan blue dye exclusion. Cells that were at least 90% viable were used in this study. Cells were cultured in a humidified 5% CO_2 incubator at 37 °C.

4.4. Histological analysis

After intravenous administration of snPt, mouse livers were removed and fixed with 4% paraformaldehyde. Thin tissue sections were stained with hematoxylin and eosin for histological observation.

4.5. Biochemical assay

Serum alanine aminotransferase (ALT) and aspartate aminotransferase (AST) were measured using commercially available kits (WAKO Pure Chemical, Osaka, Japan), respectively. Interleukin-6 (IL-6) levels were measured with an ELISA kit (BioSource International, Camarillo, CA, USA). These assays were performed according to the manufacturer's protocols.

4.6. Cell viability assay

Cell viability was determined using WST-8 (Nacalai Tesque, Osaka, Japan), according to the manufacturer's protocol. Briefly, 1×10^4 cells/well were seeded on a 96 well plate at 37 °C overnight. After 24 h of treatment with snPt, WST-8 reagent was added to each well. The plate was incubated for 1 h at 37 °C and assessed at an absorbance of 450 nm by a plate reader. Obtained data were normalized to the control group, which was designated as 100%.

4.7. Statistical analysis

Data are presented as means ± SD. Statistical analysis was performed by student's t-test. $P < 0.05$ was considered statistically significant.

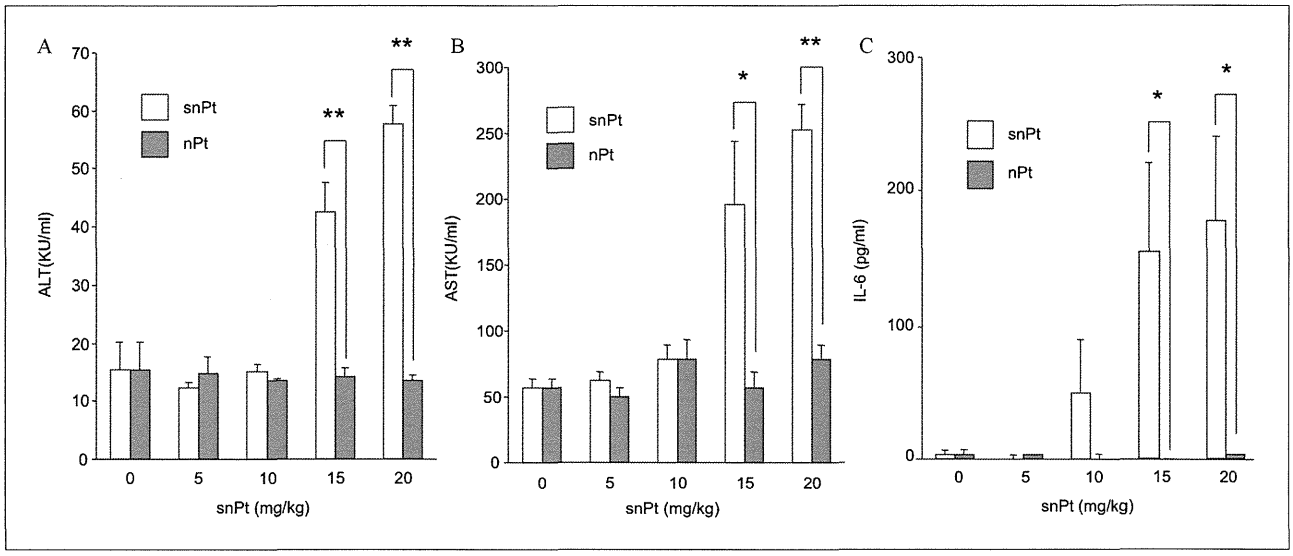

Fig. 5: Effect of particle size of platinum on liver injury. snPt or nPt was intravenously injected into mice at the indicated doses. Blood was recovered at 24 h after injection. Serum ALT (A), AST (B) and IL-6 (C) levels were measured. Data are means ± SEM (n = 3). *Significant difference between the snPt- and nPt-treated groups (*, $p < 0.05$, **, $p < 0.01$)

Acknowledgements: The authors thank all members of our laboratory for useful comments. This study was partly supported by a grant from the Ministry of Health, Labour, and Welfare of Japan.

References

Ai J, Biazar E, Jafarpour M, Montazeri M, Majdi A, Aminifard S, Zafari M, Akbari HR, Rad HG (2011) Nanotoxicology and nanoparticle safety in biomedical designs. Int J Nanomed 6: 1117–1127.

Almeida JP, Chen AL, Foster A, Drezek R (2011) *In vivo* biodistribution of nanoparticles. Nanomedicine (Lond) 6: 815–835.

Ariga K, Hu X, Mandal S, Hill JP (2010) By what means should nanoscaled materials be constructed: molecule, medium, or human? Nanoscale 2: 198–214.

Baughman RH, Zakhidov AA, de Heer WA (2002) Carbon nanotubes–the route toward applications. Science 297: 787–792.

Brabec V, Kasparkova J (2005) Modifications of DNA by platinum complexes. Relation to resistance of tumors to platinum antitumor drugs. Drug Resist Updat 8: 131–146.

Cho WS, Cho M, Jeong J, Choi M, Cho HY, Han BS, Kim HO, Lim YT, Chung BH, Jeong J (2009) Acute toxicity and pharmacokinetics of 13 nm-sized PEG-coated gold nanoparticles. Toxicol Appl Pharmacol 236: 16–24.

Clift MJ, Rothen-Rutishauser B, Brown DM, Duffin R, Donaldson K, Proudfoot L, Guy K, Stone V (2008) The impact of different nanoparticle surface chemistry and size on uptake and toxicity in a murine macrophage cell line. Toxicol Appl Pharmacol 232: 418–427.

Daugaard G (1990) Cisplatin nephrotoxicity: experimental and clinical studies. Dan Med Bull 37: 1–12.

Folkmann JK, Risom L, Jacobsen NR, Wallin H, Loft S, Moller P (2009) Oxidatively damaged DNA in rats exposed by oral gavage to C60 fullerenes and single-walled carbon nanotubes. Environ Health Perspect 117: 703–708.

Furuyama A, Kanno S, Kobayashi T, Hirano S (2009) Extrapulmonary translocation of intratracheally instilled fine and ultrafine particles via direct and alveolar macrophage-associated routes. Arch Toxicol 83: 429–437.

Gehrke H, Pelka J, Hartinger CG, Blank H, Bleimund F, Schneider R, Gerthsen D, Brase S, Crone M, Turk M, Marko D (2011) Platinum nanoparticles and their cellular uptake and DNA platination at non-cytotoxic concentrations. Arch Toxicol 85: 799–812.

Horie M, Kato H, Endoh S, Fujita K, Nishio K, Komaba LK, Fukui H, Nakamura A, Miyauchi A, Nakazato T, Kinugasa S, Yoshida Y, Hagihara Y, Morimoto Y, Iwahashi H (2011) Evaluation of cellular influences of platinum nanoparticles by stable medium dispersion. Metallomics 3: 1244–1252.

Ji Z, Zhang D, Li L, Shen X, Deng X, Dong L, Wu M, Liu Y (2009) The hepatotoxicity of multi-walled carbon nanotubes in mice. Nanotechnology 20: 445101.

Jiang J, Oberdorster G, Elder A, Gelein R, Mercer P, Biswas P (2008) Does Nanoparticle Activity Depend upon Size and Crystal Phase? Nanotoxicology 2: 33–42.

Kajita M, Hikosaka K, Iitsuka M, Kanayama A, Toshima N, Miyamoto Y (2007) Platinum nanoparticle is a useful scavenger of superoxide anion and hydrogen peroxide. Free Radic Res 41: 615–626.

Nabeshi H, Yoshikawa T, Arimori A, Yoshida T, Tochigi S, Hirai T, Akase T, Nagano K, Abe Y, Kamada H, Tsunoda S, Itoh N, Yoshioka Y, Tsutsumi Y (2011) Effect of surface properties of silica nanoparticles on their cytotoxicity and cellular distribution in murine macrophages. Nanoscale Res Lett 6: 93.

Nel A, Xia T, Madler L, Li N (2006) Toxic potential of materials at the nanolevel. Science 311: 622–627.

Nishimori H, Kondoh M, Isoda K, Tsunoda S, Tsutsumi Y, Yagi K (2009) Histological analysis of 70-nm silica particles-induced chronic toxicity in mice. Eur J Pharm Biopharm 72: 626–629.

Nishimori H, Kondoh M, Isoda K, Tsunoda S, Tsutsumi Y, Yagi K (2009) Silica nanoparticles as hepatotoxicants. Eur J Pharm Biopharm 72: 496–501.

Oberdorster G (2010) Safety assessment for nanotechnology and nanomedicine: concepts of nanotoxicology. J Intern Med 267: 89–105.

Oberdorster G, Oberdorster E, Oberdorster J. Nanotoxicology: an emerging discipline evolving from studies of ultrafine particles (2005) Environ Health Perspect 113: 823–839.

Oberdorster G, Sharp Z, Atudorei V, Elder A, Gelein R, Kreyling W, Cox C (2004) Translocation of inhaled ultrafine particles to the brain. Inhal Toxicol 16: 437–445.

Onizawa S, Aoshiba K, Kajita M, Miyamoto Y, Nagai A (2009) Platinum nanoparticle antioxidants inhibit pulmonary inflammation in mice exposed to cigarette smoke. Pulm Pharmacol Ther 22: 340–349.

Park EJ, Kim H, Kim Y, Park K (2010) Intratracheal instillation of platinum nanoparticles may induce inflammatory responses in mice. Arch Pharm Res 33: 727–735.

Patra CR, Bhattacharya R, Mukhopadhyay D, Mukherjee P (2010) Fabrication of gold nanoparticles for targeted therapy in pancreatic cancer. Adv Drug Deliv Rev 62: 346–361.

Pelka J, Gehrke H, Esselen M, Turk M, Crone M, Brase S, Muller T, Blank H, Send W, Zibat V, Brenner P, Schneider R, Gerthsen D, Marko D (2009) Cellular uptake of platinum nanoparticles in human colon carcinoma cells and their impact on cellular redox systems and DNA integrity. Chem Res Toxicol 22: 649–659.

Seglen PO (1976) Preparation of isolated rat liver cells. Methods Cell Biol 13: 29–83.

Service RF. U.S. nanotechnology (2007) Health and safety research slated for sizable gains. Science 315: 926.

Singh S, Shi T, Duffin R, Albrecht C, van Berlo D, Hohr D, Fubini B, Martra G, Fenoglio I, Borm PJ, Schins RP (2007) Endocytosis, oxidative stress and IL-8 expression in human lung epithelial cells upon treatment with fine and ultrafine TiO2: role of the specific surface area and of surface methylation of the particles. Toxicol Appl Pharmacol 222: 141–151.

Watanabe A, Kajita M, Kim J, Kanayama A, Takahashi K, Mashino T, Miyamoto Y (2009) *In vitro* free radical scavenging activity of platinum nanoparticles. Nanotechnology 20: 455105.

Zhu MT, Feng WY, Wang B, Wang TC, Gu YQ, Wang M, Wang Y, Ouyang H, Zhao YL, Chai ZF (2008) Comparative study of pulmonary responses to nano- and submicron-sized ferric oxide in rats. Toxicology 247: 102–111.

molecular pharmaceutics

Brief Article

pubs.acs.org/molecularpharmaceutics

Involvement of Ca^{2+} and ATP in Enhanced Gene Delivery by Bubble Liposomes and Ultrasound Exposure

Daiki Omata,[†] Yoichi Negishi,*[,†] Sho Yamamura,[†] Shoko Hagiwara,[†] Yoko Endo-Takahashi,[†] Ryo Suzuki,[‡] Kazuo Maruyama,[‡] Motoyoshi Nomizu,[§] and Yukihiko Aramaki[†]

[†]Department of Drug Delivery and Molecular Biopharmaceutics, School of Pharmacy, Tokyo University of Pharmacy and Life Sciences, Hachioji, Tokyo 192-0392, Japan

[‡]Department of Biopharmaceutics, School of Pharmaceutical Sciences, Teikyo University, Sagamihara, Kanagawa 252-5195, Japan

[§]Department of Clinical Biochemistry, School of Pharmacy, Tokyo University of Pharmacy and Life Sciences, Hachioji, Tokyo 192-0392, Japan

ABSTRACT: Recently, we reported the accelerated gene transfection efficiency of laminin-derived AG73-peptide-labeled polyethylene glycol-modified liposomes (AG73-PEG liposomes) and cell penetrating TAT-peptide labeled PEG liposomes using PEG-modified liposomes, which trap echo-contrast gas, "Bubble liposomes" (BLs), and ultrasound (US) exposure. BLs and US exposure were reported to enhance the endosomal escape of AG73-PEG liposomes, thereby leading to increased gene expression. However, the mechanism behind the effect of BLs and US exposure on endosomes is not well understood. US exposure was reported to induce an influx of calcium ions (Ca^{2+}) by enhancing permeability of the cell membrane. Therefore, we examined the effect of Ca^{2+} on the endosomal escape and transfection efficiency of AG73-PEG liposomes, which were previously enhanced by BLs and US exposure. For cells treated with EGTA, the endosomal escape and gene expression of AG73-PEG liposomes were not enhanced by BLs and US exposure. Similarly, transfection efficiency of the AG73-PEG liposomes in ATP-depleted cells was not enhanced. Our results suggest that Ca^{2+} and ATP are necessary for the enhanced endosomal escape and gene expression of AG73-PEG liposomes by BLs and US exposure. These findings may contribute to the development of useful techniques to improve endosomal escape and achieve efficient gene transfection.

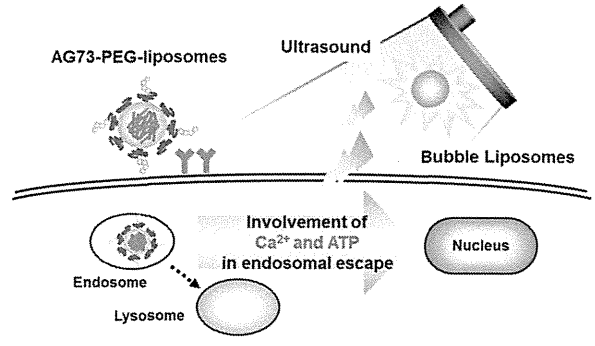

KEYWORDS: *AG73 peptide, atp, Bubble liposomes, calcium ions, gene delivery, endosomal escape, ultrasound*

INTRODUCTION

For successful gene therapy, various nonviral vectors such as lipid- and polymer-based carriers have been developed. However, they generally have relatively low transfection efficiencies, which need to be overcome.[1] Recent reports have emphasized the importance of subcellular and intracellular trafficking of gene delivery carriers. To achieve efficient gene transfection, carriers must overcome several steps including cellular internalization, endosomal escape, nuclear transfer and intracellular transcription.[2,3] Of these steps, endosomal escape is considered one of the most important, because most carriers are internalized into cells via an endocytic pathway. When escape from endosomes is impossible, the genes are degraded in lysosomes. Indeed, some groups have developed carriers and protocols that involve monitoring functions, such as pH sensitivity, temperature dependence, or photosensitivity, to deliver genes to the cytosol from endosomes.[4−7]

Previously, we developed laminin-derived AG73 peptide-labeled polyethylene glycol (PEG)-modified liposomes (AG73-PEG liposomes) as tumor targeted gene delivery carriers.[8] We also reported that the transfection efficiency of AG73-PEG liposomes and TAT-PEG liposomes, which were labeled with a TAT peptide (a cell penetrating peptide derived from human immunodeficiency virus trans-acting transcriptional activator), could be accelerated by PEG-modified liposomes, which trap echo-contrast gas, "Bubble liposomes" (BLs), and ultrasound (US) exposure.[9,10] BLs and US exposure enhanced the endosomal escape of AG73-PEG liposomes and TAT-PEG liposomes, leading to increased gene expression. However, the mechanism behind the effect of BLs and US exposure on endosomes and the resulting enhanced endosomal escape of carriers is not well understood. To promote this method as a more useful gene delivery tool, it is necessary to understand the detailed interactions at a fundamental level.

US pressure above a certain threshold can cause oscillating bubbles to undergo a violent collapse known as inertial cavitation. Microbubbles can be the nuclei of cavitation, and

Received: November 28, 2011
Revised: January 26, 2012
Accepted: March 2, 2012
Published: March 2, 2012

subsequent US exposure can induce more efficient cavitation. Inertial cavitation is thought to cause transient disruptions in cell membranes, which enable the transport of extracellular molecules into cells.[11−16] However, US exposure has also induced several biological effects, such as bone fracture healing, wound healing, and induction of apoptosis.[17−19] Moreover, the induced influx of calcium ions, the generation of reactive oxygen species, or the activation of some signals at a cellular level can be attributed to US exposure.[20−23]

Calcium ions (Ca^{2+}) have important roles in cells and are involved in various events such as cell proliferation and cell death.[24,25] US exposure induces the influx of Ca^{2+} by enhancing permeability of the cell membrane. Ca^{2+} also adjusts endosomal acidification and vesicle fusion.[26−29] Therefore, we focused on Ca^{2+} and hypothesized that BLs and US enhance the endosomal escape of gene delivery carriers via Ca^{2+} influx. We also investigated the involvement of ATP in enhanced gene delivery. In this study, we examined the effect of Ca^{2+} and ATP on the endosomal escape and transfection efficiency of AG73-PEG liposomes enhanced by BLs and US exposure.

EXPERIMENTAL SECTION

Materials. The pcDNA3-Luc plasmid, derived from pGL3-basic (Promega, Madison, WI), is an expression vector encoding the firefly luciferase gene under the control of a cytomegalovirus promoter. EGTA (ethylene glycol-bis(2-aminoethyl ether)-*N,N,N′,N′*-tetraacetic acid) was purchased from Sigma (St. Louis, MO). NaF and NaN_3 were purchased from Wako Pure Chemical Industries, Ltd. (Osaka, Japan). Antimycin A was purchased from Enzo Life Sciences, Inc. . (Farmingdale, NY). Alexa Fluor 488-conjugated transferrin was purchased from Molecular Probes, Inc. (Eugene, OR).

Cell Lines and Cultures. A 293T human embryonic kidney carcinoma cell line, stably overexpressing syndecan-2 (293T-Syn2 cell), was cultured in Dulbecco's modified Eagle's medium (DMEM; Kohjin Bio Co. Ltd., Tokyo, Japan), supplemented with 10% fetal bovine serum (FBS; Equitech Bio Inc., Kerrville, TX), penicillin (100 U/mL), streptomycin (100 μg/mL), and puromycin (0.4 μg/mL), at 37 °C in humidified 5% CO_2 atmosphere.

Preparation of AG73-PEG Liposomes. The Cys-AG73 peptide (CGG-RKRLQVQLSIRT) was synthesized manually using the 9-fluorenylmethoxycarbony (Fmoc)-based solid-phase strategy. The peptide was prepared in the COOH-terminal amide form and purified by reverse phase high-performance liquid chromatography. AG73-labeled PEG liposomes were prepared by the hydration method. The pDNA was diluted to a concentration of 0.1 mg/mL in 10 mM HEPES buffer (pH 7.4) and was condensed using 0.1 mg/mL poly-L-lysine (PLL); (SIGMA-Aldrich Co., St. Louis, MO). The complex of pDNA-PLL was added to a lipid film composed of 1,2-dioleoyl-*sn*-glycero-3-phospho-*rac*-1-glycerol (DOPG) (AVANTI Polar Lipids Inc., Alabaster, AL), 1,2-dioleoyl-*sn*-glycero-3-phosphoethanolamine (DOPE) (AVANTI Polar Lipids Inc., Alabaster, AL), and 1,2-distearoyl-*sn*-glycero-3-phosphatidylethanolamine-polyethylene glycol-maleimide (DSPE-PEG_{2000}-Mal) (NOF Corporation, Tokyo, Japan) in a molar ratio of 2:9:0.57 followed by incubation for 10 min at room temperature to hydrate the lipids. The solution was sonicated for 5 min in a bath-type sonicator (42 kHz, 100 W) (BRANSONIC 2510J-DTH, Bransoni Ultrasonic Co., Danbury, CT). For coupling, AG73 peptide, at a molar ratio of 5-fold DSPE-PEG_{2000}-Mal, was added to the PEG liposomes, and the mixture was incubated for 6 h at room temperature to conjugate the cysteine of Cys-AG73 peptide to the maleimide of the PEG liposomes using a thioether bond. The resulting AG73-peptide-conjugated PEG liposomes (AG73-PEG liposomes) were dialyzed to remove any excess peptide. AG73-PEG liposomes were modified with 5 mol % PEG and 3 mol % peptides.

Preparation of Bubble Liposomes. PEG liposomes composed of 1,2-dipalmitoyl-*sn*-glycero-3-phosphocholine (DPPC) (NOF Corporation, Tokyo, Japan) and 1,2-distearoyl-*sn*-glycero-3-phosphatidylethanolamine-polyethylene glycol (DSPE-PEG_{2000}-OMe) (NOF Corporation, Tokyo, Japan) in a molar ratio of 94:6 were prepared by a reverse-phase evaporation method. In brief, all reagents were dissolved in 1:1 (v/v) chloroform/diisopropyl ether. Phosphate buffered saline was added to the lipid solution, and the mixture was sonicated and then evaporated at 47 °C. The organic solvent was completely removed, and the size of the liposomes was adjusted to less than 200 nm using extruding equipment and a sizing filter (pore size: 200 nm) (Nuclepore Track-Etched Membrane, GE Healthcare, U.K.). The lipid concentration was measured using a Phospholipid C test Wako (Wako Pure Chemical Industries, Ltd., Osaka, Japan). BLs were prepared from liposomes using perfluoropropane gas (Takachio Chemical Ind. Co. Ltd., Tokyo, Japan). First, 2 mL sterilized vials containing 0.8 mL of the liposome suspension (lipid concentration: 1 mg/mL) were filled with perfluoropropane gas, capped, and then pressurized with a further 3 mL of perfluoropropane gas. The vials were placed in a bath-type sonicator (42 kHz, 100 W) (BRANSONIC 2510j-DTH, Branson Ultrasonics Co., Danbury, CT) for 5 min to form BLs.

Gene Transfection by AG73-PEG Liposomes with BLs and US Exposure. Two days before the experiments, 293T-Syn2 cells (1×10^5) were seeded in a 48-well plate. The cells were treated with AG73-PEG liposomes (encapsulating pDNA: 3 μg/mL) in serum-free medium for 4 h at 37 °C. The cells were washed twice with Ca^{2+}-free DMEM containing 10 mM EGTA. To deplete ATP, the cells were treated with NaN_3 (0.1%), NaF (10 mM), and antimycin A (1 μg/mL) for 30 min, and then the BLs were added. Within 2 min, US exposure was applied through a 6 mm diameter probe placed in the well (frequency, 2 MHz; duty, 50%; burst rate, 2 Hz; intensity, 1.0 W/cm^2; time, 10 s). A Sonopore 3000 (NEPA GENE, CO., Ltd., Chiba, Japan) was used to generate the US. The cells were transferred to fresh medium and cultured for 20 h, and then luciferase activity was determined.

Measurement of Luciferase Expression. Cell lysates were prepared with lysis buffer (0.1 M Tris-HCl pH 7.8, 0.1% Triton X-100, and 2 mM EDTA). Luciferase activity was measured as relative light units (RLU) per mg of protein using a luciferase assay system (Promega, Madison, WI) and a luminometer (LB96 V, Belthold Japan Co. Ltd., Tokyo, Japan).

Assessment of Localization of pDNA and Transferrin. The 293T-Syn2 cells (7×10^4) were seeded two days before the experiments. The cells were treated with AG73-PEG liposomes (Cy3-labeled pDNA: 3 μg/mL) and Alexa Fluor 488-conjugated transferrin (50 μg/mL) for 4 h at 37 °C. After incubation, the cells were washed, and the BLs (120 μg/mL) were added. Then, US exposure was applied (frequency, 2028 kHz; duty, 50%; burst rate, 2.0 Hz; intensity, 1.0 W/cm^2; time, 10 s). To assess the involvement of Ca^{2+} and ATP, the cells were treated as described in the above section. Subsequently, the cells were incubated for 10 min and then fixed with 4%

paraformaldehyde for 1 h at 4 °C followed by visualization using confocal laser scanning microscopy (CLSM). To differentiate the AG73-PEG liposomes internalized into the cytoplasm following attachment to the surface of the cell membrane, the cytoplasm was distinguished from the cell membrane as shown previously.[9,10,30,31] The rate of colocalization of Cy3-labeled pDNA with Alexa Fluor 488-conjugated transferrin was quantified as follows: amount of colocalization (%) = Cy3 $pixels_{colocalization}$/Cy3 $pixels_{total}$ × 100, where Cy3 $pixels_{colocalization}$ represents the number of Cy3 pixels colocalizing with Alexa Fluor 488-conjugated transferrin and Cy3 $pixels_{total}$ represents the total number of Cy3 pixels.

Assessment of Localization of pDNA and lamp-2. The 293T-Syn2 cells were first treated with AG73-PEG liposomes (Cy3-lableled pDNA: 3 μg/mL) for 4 h at 37 °C and then with BLs and US exposure. To assess the involvement of Ca^{2+} and ATP, cells were treated as described in the above section. Subsequently, the cells were incubated for 1 h and then fixed with 4% paraformaldehyde for 1 h at 4 °C. The cells were washed with PBS and permeabilized for 5 min in 0.2% saponin, followed by treatment with 10% goat serum in PBS. Finally, the cells were incubated with anti-lamp2 Ab (Santa Cruz Biotechnology, Inc., Santa Cruz, CA) overnight at 4 °C and treated with Alexa Fluor 488-conjugated secondary Ab (Invitrogen Co., Carlsbad, CA) for 1 h at room temperature in the dark. Then, CLSM and analysis was performed as described in the above section.

RESULTS AND DISCUSSION

In previous reports, we have showed that BLs and US exposure could enhance endosomal escape and gene transfection of AG73-PEG liposomes. We have proposed the mechanism that the cavitation induced in the outside of cells by US exposure and BLs could affect endosomes, and then AG73-PEG liposomes internalized by endocytosis escaped from endosomes, leading to enhanced gene expression. It have been also confirmed that AG73-PEG liposomes could not be introduced into cytoplasm directly through the cell membrane after the US-mediated disruption of BLs. However, the exact mechanism of accelerated endosomal escape of carriers was not clear. US exposure induces the influx of Ca^{2+} by enhancing permeability of the cell membrane.[21] In addition, Ca^{2+} adjusts endosomal acidification and vesicle fusion.[26−29] Therefore, to evaluate the mechanism by which BLs and US exposure could promote the endosomal escape of AG73-PEG liposomes, we examined the effect of Ca^{2+} on the endosomal escape and transfection efficiency of AG73-PEG liposomes enhanced by BLs and US exposure. ATP is involved in various reactions, such as acidification of endosomes, intracellular trafficking of vesicles and fusion of vesicles.[26] We also investigated the involvement of ATP-dependent processes in enhanced gene delivery.

First, to evaluate the involvement of Ca^{2+} and ATP in gene expression enhanced by BLs and US exposure, we examined the effect of Ca^{2+} and ATP on gene expression efficiency of AG73-PEG liposomes using 293T-Syn2 cells. The cells were incubated with AG73-PEG liposomes containing pcDNA3-Luc, and then treated with BLs and US exposure. After 20 h incubation, luciferase activity was assayed. BLs and US exposure enhanced the luciferase activity of AG73-PEG liposomes by approximately 60-fold compared to that of AG73-PEG liposomes alone.[9] By contrast, when the cells were treated with 10 mM EGTA before the treatment of BLs and US exposure, the enhancement ratio of luciferase activity by BLs and US exposure was decreased. To examine the effect of ATP on gene transfection efficiency, the cells were treated with NaN_3, NaF, and antimycin A to deplete ATP. The subsequent luciferase assay showed insignificant enhancement by BLs and US exposure. Conversely, when cells were treated with AG73-PEG liposomes alone, luciferase activity was not affected by Ca^{2+} and ATP depletion (Figure 1). These results suggest that

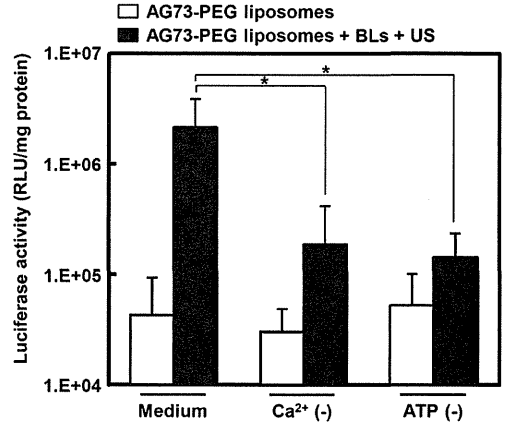

Figure 1. Effects of Ca^{2+} and ATP on gene expression by AG73-PEG liposomes with BLs and US exposure. 293T-Syn2 cells were treated with AG73-PEG liposomes for 4 h at 37 °C, and then cells were washed twice with Ca^{2+}-free DMEM containing 10 mM EGTA for a depleted Ca^{2+} condition. ATP was depleted by pretreating cells for 30 min before US exposure with 1 μg/mL antimycin A, 10 mM NaF, and 0.1% NaN_3. BLs (120 μg/mL) were added to cells followed by immediate US exposure. After replacement with fresh medium, the cells were cultured for 20 h and luciferase activity was determined. The data are shown as the means ± SD (n = 4). *p < 0.05.

Ca^{2+} and ATP may be necessary to enhance gene transfection efficiency of AG73-PEG liposomes by BLs and US exposure. On the other hand, it is reported that extracellular Ca^{2+} plays important roles to repair the cell membrane disruption and maintain cell survival.[32] Therefore, we examined the cell viability in Ca^{2+}-depleted condition. As a result, in this condition, the cell viability had almost no difference in the treatment with or without BLs and US exposure (data not shown). This result suggested that the decreased enhancement ratio of luciferase activity by the treatment of BLs and US exposure in Ca^{2+}-depleted condition was not due to a change of cell viability.

Recent reports have emphasized the importance of subcellular and intracellular trafficking of gene delivery carriers.[2,3] Among the several steps involeved, endosomal escape is considered one of the most important. In previous study, we have reported that enhanced endosomal escape of AG73-PEG liposomes by BLs and US exposure could increase gene expression.[9] Therefore, we evaluated the involvement of Ca^{2+} and ATP on the endosomal escape of gene delivery carriers. We examined the effects of Ca^{2+} and ATP on localization of pDNA encapsulated in AG73-PEG liposomes and transferrin, as an endosome marker,[33] by confocal microscopy. BLs and US exposure enhanced the endosomal escape of AG73-PEG liposomes and decreased the ratio of colocalization of pDNA and transferrin.[9] The 293T-Syn2 cells were first incubated with AG73-PEG liposomes containing Cy3-labeled pDNA and Alexa Fluor 488-conjugated transferrin and then treated with BLs and US exposure. The cells were observed by confocal microscopy to assess the colocalization of